Investigation of converter failure in wind turbines

A pre-study

Elforsk report 12:58

Katharina Fischer, Thomas Stalin, Hans Ramberg,
Torbjörn Thiringer, Jan Wenske, Robert Karlsson

November 2012

Investigation of converter failure in wind turbines

A pre-study

Elforsk report 12:58

Katharina Fischer, Thomas Stalin, Hans Ramberg,
Torbjörn Thiringer, Jan Wenske, Robert Karlsson November 2012

Preface

Frequent failure of the power-electronic converters in offshore wind turbines is a problem with considerable impact on the turbine availability, and therefore the revenue from production, as well as on the maintenance cost.

A project was therefore started as project V-375," ConFail", Investigation of converter failure in wind turbines. A project within the Swedish wind energy research program "Vindforsk – III.

The project aims at increasing the knowledge concerning the failure modes and the causes of the converter failures, as a basis for the identification of suitable countermeasures and potential further investigation needs.

The project was carried out by Katharina Fischer, Torbjörn Thiringer and Robert Karlsson at Chalmers University of Technology in close collaboration with Thomas Stalin, Vattenfall Vindkraft AB, and an expert group involving Hans Ramberg, Volvo Car Corporation, Jan Wenske, Fraunhofer IWES, and Hector Zelaya, ABB Corporate Research.

Vindforsk – III is funded by ABB, Arise windpower, AQSystem, E.ON Elnät, E.ON Vind Sverige, EnergiNorge, Falkenberg Energi, Fortum, Fred. Olsen Renwables, Gothia wind, Göteborg Energi, HS Kraft, Jämtkraft, Karlstads Energi, Luleå Energi, Mälarenergi, o2 Vindkompaniet, Rabbalshede Kraft, Skellefteå Kraft, Statkraft, Stena Renewable, Svenska Kraftnät, Tekniska Verken i Linköping, Triventus, Wallenstam, Varberg Energi, Vattenfall Vindkraft, Vestas Northern Europe, Öresundskraft and the Swedish Energy Agency.

Stockholm November 2012

Anders Björck

Program manager Vindforsk-III

Electricity- and heatproduction, Elforsk

Acknowledgments by the authors

Valuable comments on the work and the final report have been given by the project participants and expert-group members named above as well as by Anders Björck, Elforsk. The committed contributions of these persons to the project are most kindly acknowledged.

In addition, the authors would like to thank Urban Axelsson, Poul-Erik Amby Christensen, Mogens Forsom, Lars Höjholt, Jan Jørgensen, Mads Kristian Pedersen and Tor Söderlund at Vattenfall for valuable discussions and/or technical support to the project.

To Tusitha Abeyasekera, Vestas, thanks for contributing to the root-cause analysis carried out within the project.

The climate data used in this work was provided by the Swedish Meteorological and Hydrological Institut (SMHI) and the Danish Meteorological Institute (DMI). Parts of the investigation of converter hardware were carried out at Swerea IVF, Göteborg.

The considerable in-kind contribution of Vattenfall and Volvo Car Corporation to this project is particularly acknowledged.

Sammanfattning

En omfattande analys av omriktarspecifik fel- och alarmdata, bland annat en undersökning av sambandet mellan fel med olika miljöfaktorer såsom omgivningstemperatur, relativ luftfuktighet, vindhastighet och blixtnedslag har genomförts i detta projekt. Denna har kompletterats med en litteraturstudie fokuserad på de huvudsakligen drabbade komponenterna, felmekanismerna och felorsakerna i omvandlare i allmänhet samt i vindkraftverk i synnerhet. Vidare har de aktuella on-site driftsförhållanden av omriktarna baserat på SCADA-data samt med data som samlats in i omriktarskåpen på enstaka turbiner med hjälp av temperatur- och fuktighetsloggare, termosensitiv tejp och vibrationssensorer analyserats. Slutligen har även ett antal utbytta omriktarmoduler undersökts med hjälp av elektriska mätningar och metoder för 'forensisk' analys.

Resultaten visade på att det klassiska förslitningsfenomenet med bondtrådar som lossar från IGBT-chippen inte var något problem. Tester utförda inom projektet visade att dessa satt väl förankrade. Speciellt för DFIG-maskiner, där IGBT-er kan utsättas för mycket termisk cykling vid drift nära synkront varvtal kan detta vara ett problem.
Av de kraftverk som undersöktes i studien så var havsbaserade vindkraftverk inte överrepresenterade felmässigt.
En starkt korrelation mellan blixtnedslag och omriktarfel kunde observeras. Detta understöddes av den 'forensiska' analysen, där moduler uppvisade just denna problemorsak. Döda insekter kunde upptäckas i närheten till modulerna, huruvida dessa kan orsaka överslag är dock osäkert, men det rekommenderas likväl att vidta åtgärder i kraftverk där insektsmängden är stor.
Kondensation misstänktes också vara en felorsak, rekommendationen här är att kontrollera att förvärmning fungerar på avsett vis då risk för kondensation vid ett stillestånd finns.
Dataloggning av temperaturen genomfördes april till juni 2012. Denna visade inte på några förhöjda temperaturer, och därmed ansågs förhöjd temperatur i omriktarskåpen inte vara en felorsak. Det var dock inte möjligt att avgöra om den termiska pastan mellan IGBT-erna och omriktarmodulernas kylfläns hade degraderats, vilket i så fall skulle kunna lett till förhöjd temperatur i IGBTerna likaväl.
En undersökt modul från Site B uppvisade avlagringar av salt och tillhörande korrosion. Huruvida detta salt hamnat där under transporten eller driften är okänt, dock kan det rekommenderas att åtgärder vidtas så att salt inte hamnar på modulerna.

Detta arbete har givit indikationer på felorsaker. För att mera statistiskt säkerställt kunna presentera felorsakerna, föreslås att dokumentation vid omriktarfel förbättras och analyseras tillsammans med SCADA-data. Vidare föreslås en mer omfattande forensisk analys, helst med mera bakgrundsinformation om driftsituationen för den specifika felande komponenten. Slutligen, så föreslås en mer omfattande loggning av situationen i omriktarskåp ute i turbinerna.

Summary

A comprehensive analysis of converter-specific failure and alarm data has been carried out in this project, including an investigation of the correlation between failure and different environmental factors like the ambient temperature, the relative humidity, the wind speed and the number of lightning strikes. This has been complemented with a literature study focused on the predominantly failure-affected components, the failure mechanisms and the failure causes in converters in general, and on wind-turbine specific results in particular. Furthermore, the on-site operating conditions of the converters have been assessed, based on SCADA-data analysis and data collected in the converter cabinets of selected turbines by means of temperature and humidity loggers, thermo-sensitive tape and vibration measurements. Finally, a number of replaced converter modules have been investigated by means of electrical measurements and methods of forensic analysis.

The results suggest that the classical fatigue-related phenomenon of bond-wire lift-off from the IGBT chips is not among the dominant failure mechanisms. Tests carried out within the project showed that the bond wires were well attached to the chips. Particularly in DFIG turbines, in which IGBTs can be subject to severe thermal cycling during operation close to synchronous speed, this can be a problem.

The failure-data analysis did not provide any indications that converter failure occurs more frequently at offshore sites than at onshore sites.

A strong correlation between lightning strikes and converter failure was observed. This was supported by the results of the forensic analysis, in which converter modules showed signs of electrical overstress. Dead insects were discovered inside the converter cabinets. Although there is some uncertainty how these can cause flashover, it is recommended to take countermeasures in turbines with large amounts of insects.

Another suspected cause of converter failure is condensation after longer periods of standstill; it is thus recommended to check the application and effectiveness of the present preheating routines.

Data logging of the temperature was carried out from April to June 2012. This did not reveal any abnormal temperatures, so that high temperature inside the converter cabinets is not considered a failure cause. However, it was not possible to determine if the thermal paste between IGBTs and heat sink was deteriorated, which in that case could still have led to high temperatures in the IGBTs.

One of the investigated modules from the offshore site B showed traces of salt and related corrosion. It is unclear if this salt ended up on the modules during transportation or operation. However, preventive measures are recommended in any case in order to prevent the ingress of salt into the converter modules.

This work has provided indications regarding probable failure causes. In order to obtain clearer evidence with respect to this, it is proposed that the documentation in case of converter failure is improved and that this is collected and analysed in addition to the SCADA data. Furthermore, more comprehensive forensic analysis is recommended, preferably with additional

documentation available regarding the operating conditions of the specific failed component as suggested above. Finally, an extended logging of the conditions inside of converter cabinets in the field is proposed.

Content

1 Introduction

The majority of modern wind turbines has designs allowing variable-speed operation as this has proven to significantly reduce the mechanical loading of their structures. Common generator topologies are (see e.g. [1]):

- an induction generator or a (either permanent-magnet or electrically excited) synchronous generator with a full-scale power converter (see Fig. 1a, b and d),
- a doubly-fed induction generator (DFIG) with a partially rated power converter (see Fig. 1c).

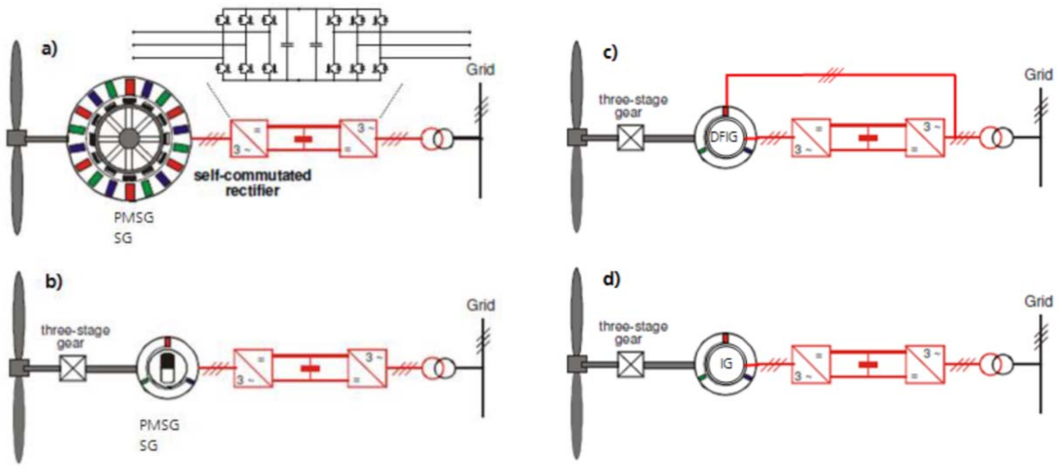

Fig. 1: Common generator topologies: synchronous generator (left) or induction generator (right) with back-to-back voltage source converter [2]

In all named topologies, power-electronic converters are required to decouple the rotational speed of the drive-train, i.e. the generator frequency, from the grid frequency.

1.1 Reliability of power-electronic converters in wind turbines

While the variable-speed capability introduced by the use of power-electronic converters in wind turbines has relieved the mechanical stress in the drive train and in this way contributes to improved reliability in this part of the wind turbine, power converters themselves are a frequent source of wind-turbine failure today: In the most recent reliability field study carried out within the EU-project RELIAWIND, Wilkinson et al. have investigated 31500 downtime events in pitch-controlled variable-speed wind turbines with rated capacity ≥850 kW [3]. According to the distribution of failure rates and average downtimes over the wind-turbine subsystems and assemblies obtained in this study, shown in Fig. 2 and Fig. 3, both the failure rate and the average downtime caused by the frequency converter are among the highest and are exceeded only by those of the pitch system. In the increasing number of offshore wind parks, the impact of a high failure rate on turbine downtime is expected to be even more severe due to the accessibility of offshore installations for repair being constrained by the wind and weather conditions. Apart from the turbine downtime and related revenue loss, converter failure is afflicted with a risk of substantial secondary damage: According to [4, 5], failures in the power electronics are a common cause of fire in wind turbines.

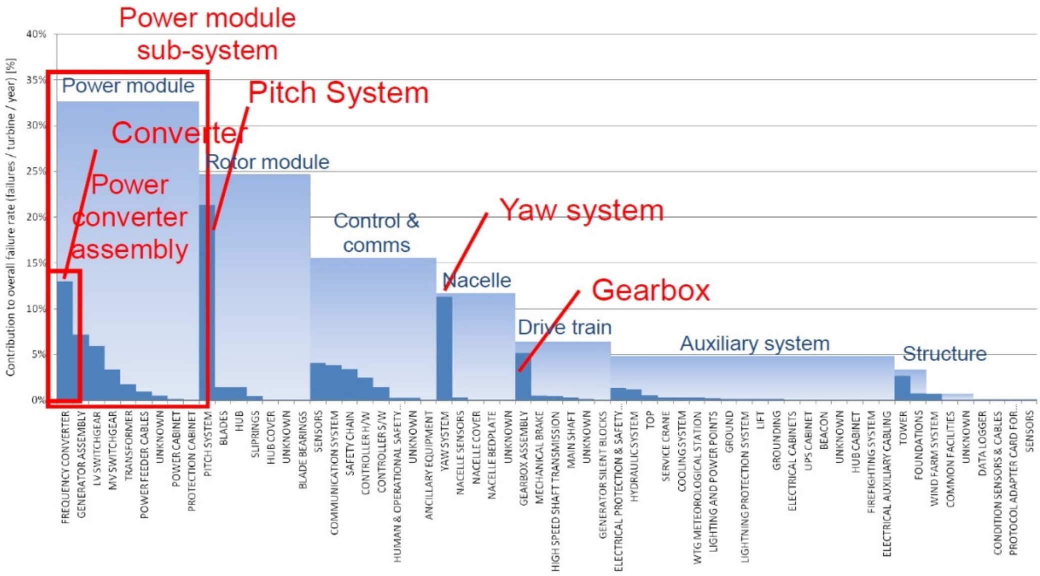

Fig. 2: Normalised failure rate of subsystems and assemblies for variable-speed wind turbines of multiple manufacturers [3]

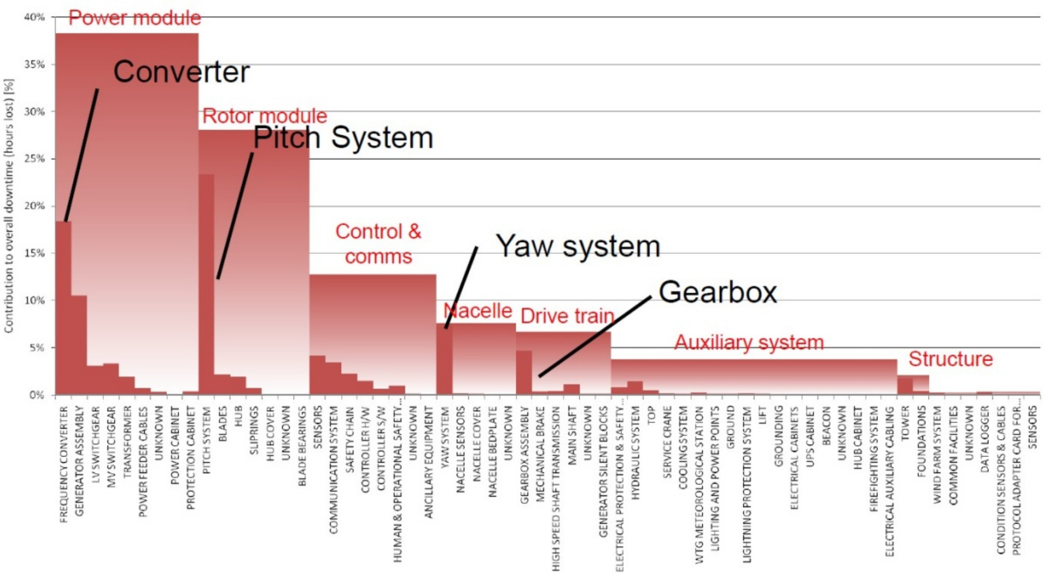

Fig. 3: Normalised hours lost per turbine per year due to faults in subsystems and assemblies for variable-speed wind turbines [3]

A similar picture concerning the converter reliability is provided by the results of Spinato et al. [6] shown in Fig. 4, which are based on an older population of turbines. In the work of these authors, the reliability of more than 6000 onshore wind turbines and their subassemblies in Denmark and Germany has been assessed using data from over 11 years (failure data sources: WindStats Germany, WindStats Denmark and LWK Schleswig-Holstein). The results confirm that particularly the converter system is subject to high failure frequencies. In addition, the authors state that both the wind-turbine generators and converters were achieving reliabilities considerably below that achieved in other industries by these assemblies.

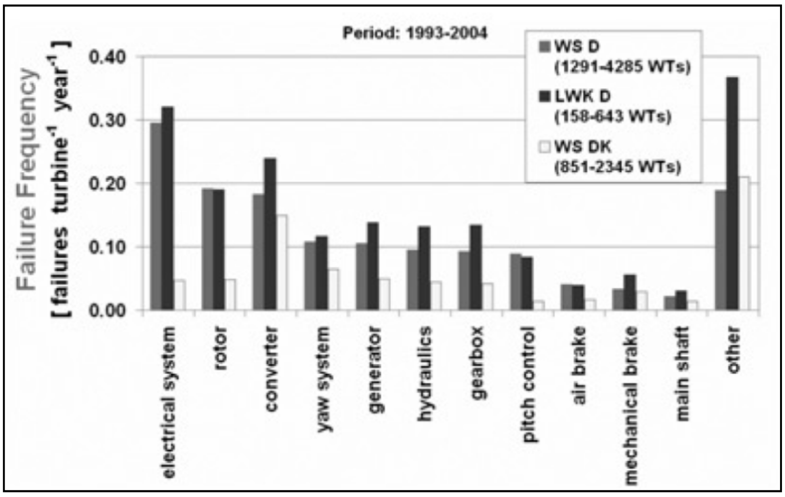

Fig. 4: Distribution of average failure rates over wind-turbine subsystems (failure data sources: WindStats Germany "WS D", WindStats Denmark "WS DK" and LWK Schleswig-Holstein "LWK D") [6]

Vattenfall confirms the high failure frequency of converters in their wind parks. The circumstances at failure give some indication about possible failure causes: Besides a suspected impact of the site (onshore vs. offshore), certain operating conditions have been observed to increase the risk of failure: Start of turbine operation after standstill periods has been observed to be particularly problematic, suggesting that condensation is a cause of failure. A speculation is that too little protection of the hardware against environmental impact (salt, moisture) is provided. Frequent failure during thunderstorms indicates a possible relation to grid disturbances and electrical overstress. Erroneous control software was named to have contributed to converter failure in the past. Operation beyond the specified operating conditions of the converter and the frequent thermal cycling caused by the operation in wind turbines are suspected to contribute to the observed converter failures. Furthermore, degradation of the thermal grease between the IGBT and the heat sink has previously been a problem in Sweden's first offshore wind park Bockstigen.

Besides this variety of potential failure causes and the present uncertainty in this respect, also the origin of failure, i.e. the fact if a failure originates from a power-electronic device, from a driver-board or e.g. from a connection between these, is not sufficiently known. A systematic investigation of the circumstances leading to failure has not been undertaken so far. This is the subject of the project described here.

1.2 Converters in wind turbines: components and properties

Independently of the generator topology, the most common converter type in modern wind turbines is the back-to-back configuration of a generator-side and a grid-side converter with a DC-voltage intermediate link, as exemplarily shown in Fig. 5 for a DFIG system, see e.g. [7] for a detailed description. Usually, IGBT switches with reverse blocking voltage ability of 1200V or 1700V are used, with a DC-voltage level between 750 and 1200V and at nominal AC-line voltages between 490 and 690V. Standard switching frequencies are in the range of several kHz. [2]

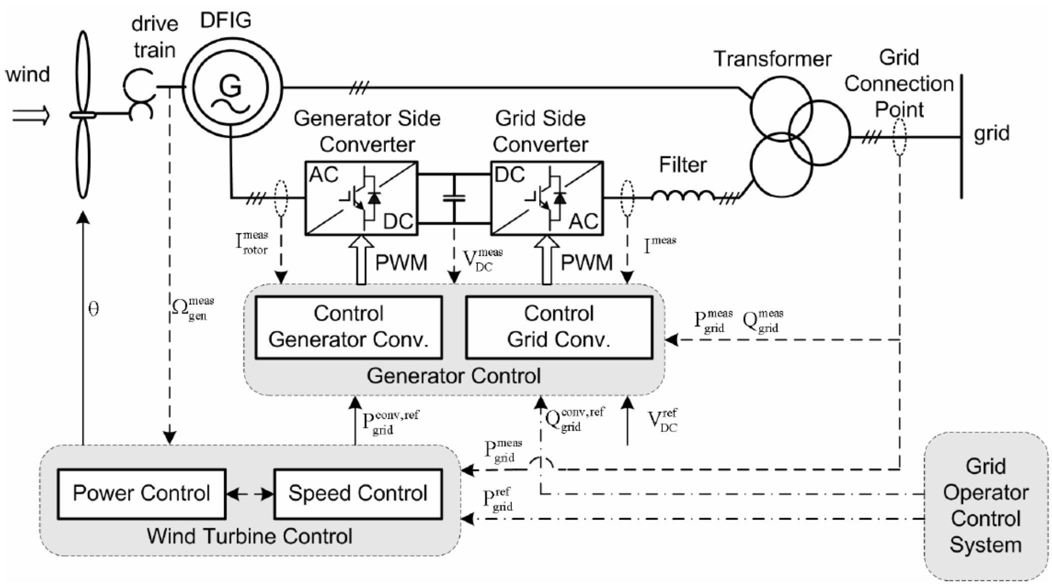

Fig. 5: Generator topology and control of a DFIG system [8]

The power-electronic converters used in wind turbines consist of so-called stacks which in turn are made of half-bridge or single-switch modules. These are mounted on heat sinks and are often water-cooled. The interface between the generator control and the IGBT power modules is provided by the driver boards. Besides the driver circuits and the modules, the abovementioned stack usually includes sensors for e.g. current and voltage measurement, monitoring and protection functions. In order to allow for the required operating currents, typically several half-bridges are connected in parallel, as e.g. in case of the 4-fold generator-side and the 3-fold grid-side module shown in Fig. 6.

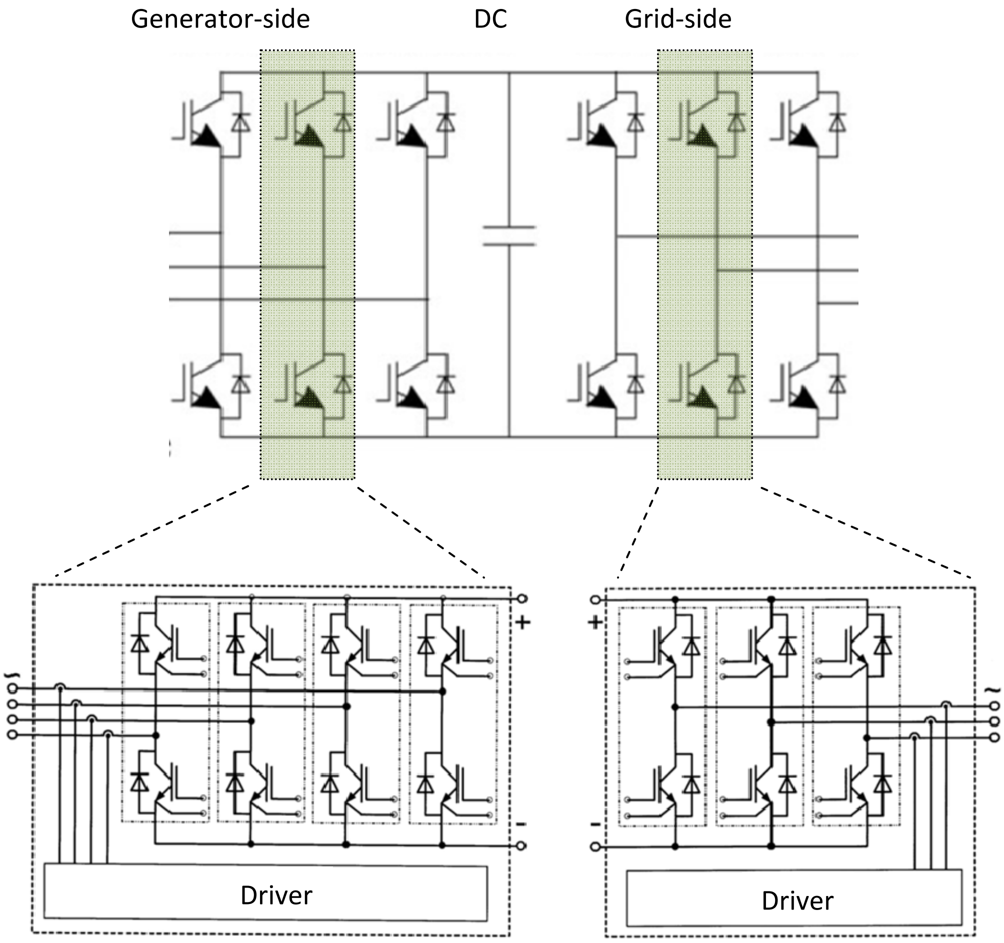

Fig. 6: Back-to-back converter of a DFIG turbine with paralleled half-bridges in each phase module to provide the required current capacity (Source: parts adopted from [11])

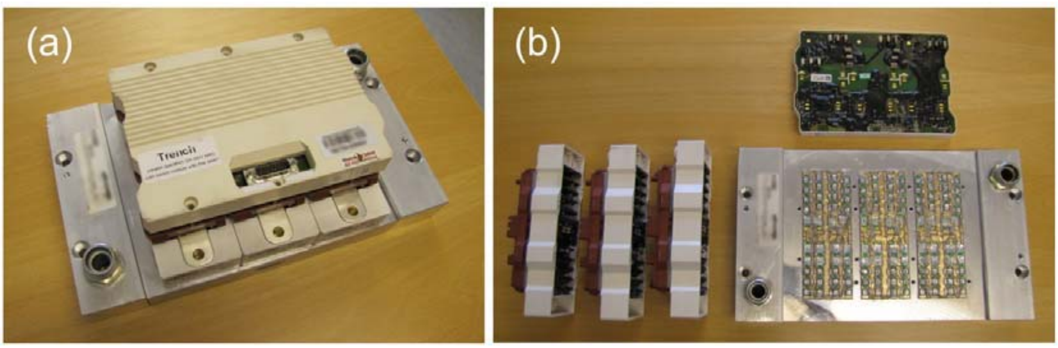

Fig. 7: Converter module used in wind turbines (3-fold, compare Fig. 6), (a) exterior view, (b) disassembled driver board, housing with connectors, power-electronic chips with heat sink

Each of these half-bridges in turn consists of a larger number of synchronously switched IGBTs and their respective freewheeling diodes to provide the overall current capacity. As pointed out by Scheuermann (2005) [9], any paralleling of half-bridges requires a certain de-rating to account for asymmetric current sharing.

In DFIG systems, the generator-side converter tends to react quite strongly in case of grid disturbances. It is therefore common to use a generator-side converter with a rated power exceeding that of the grid-side converter. In contrary in full-scale power converters, the size and rating of the generator-side and the grid-side converter are typically identical. [10]

There are two different packaging types for power devices:

The press-pack technology shown in Fig. 8 (left) has historically been applied to thyristors and rectifier-grade diodes, and is today proposed for application in medium-voltage converters in multi-MW wind turbines (see e.g. [12], see the Appendix for the definition of low-voltage and medium-voltage levels). Press-pack technology is characterised by a high reliability due to the absence of bond wires and double-sided cooling, and higher cost [13].

The second packaging structure illustrated in Fig. 8 (right) is usually referred to as module technology and is the common packaging technology in contemporary wind turbines. Herein, the power-electronic chips (IGBTs, diodes) are electrically contacted by means of bond wires. The chips are soldered to an insulating ceramic substrate, also called DCB (direct bonded copper substrate). As illustrated in Fig. 9, there are power modules with and without a base plate. In the standard case containing a base plate (Fig. 9, left), the substrate is soldered to a base plate of copper, which in turn is attached to the heat sink by means of a thermal grease. In an alternative design, e.g. used in Semikron's Skiip modules, the substrate is directly attached to the heat sink (Fig. 9, right).

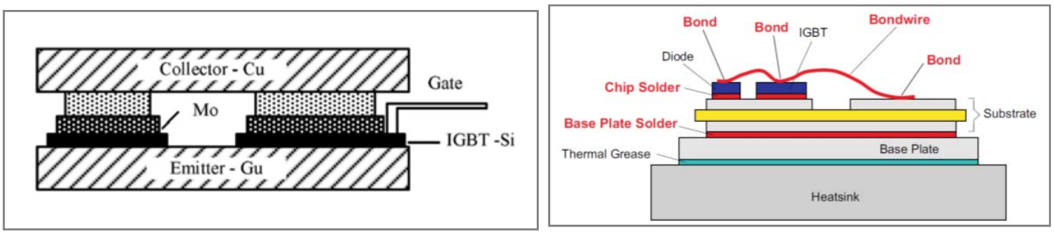

Fig. 8: Packaging technologies for power devices: press-pack technology (left, [14]) and power module (right, [11])

The IGBT chips and diodes in the investigated modules are covered with a soft potting compound, an insulating cover layer, which is used to protect electronic components from shock and vibration. Common potting compounds are pourable insulating resins like epoxies, silicones, urethanes or hybrids of these [15].

While the IGBT chips and diodes together with the ceramic substrate are well protected from the environment by means of the housing and the potting compound, the driver board is only partially protected. Located under the top cover of the module, it is accessible for air circulating in the converter cabinet, possibly carrying humidity, dust, salt or other contaminants.

The electrical contact between the power-electronic chips and the driver board is provided by means of metallic springs in the modules investigated. According to [16], spring contacts offer the advantages of easy, solder-free assembly and high reliability under environmental stress by mechanical wear, rapid temperature change or corrosive atmosphere.

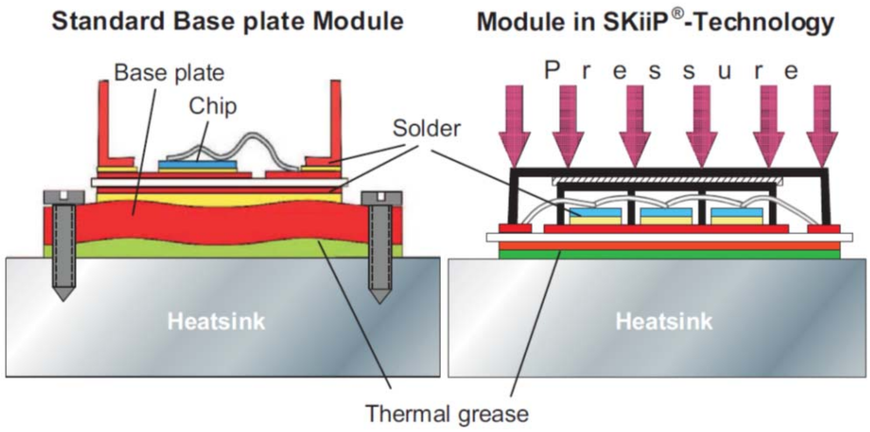

Fig. 9: Structure of power modules with (left) and without baseplate (right) [11]

The generator-side and the grid-side converter are connected via the DC link, which is equipped with a bench of capacitors. Two different types of DC link capacitors are used in wind turbines [13]:

- aluminum electrolytic capacitors, which are characterized by a high power density, low cost and low reliability; temperature is the main accelerator of ageing for this type of capacitor;
- metallised polypropylene film capacitors, which have a low power density, but can withstand higher voltages and currents, have a certain self-healing capability and provide a higher reliability; current peaks are the main ageing accelerator for this type of DC link capacitors.

2 Literature study

In Section 1.1, a short review of available statistical results from the literature regarding the failure frequency of and downtime resulting from power-electronic converters in wind turbines has been given. It has shown that the low reliability of power converters is not a problem being limited to single wind-turbine manufacturers or operators, but is a common and important challenge to be solved even in a larger perspective.

While the available statistical analyses named in Section 1.1 clearly indicate the high failure frequency of converters and their considerable contribution to turbine downtime, they do not provide any information about the technical failure modes, failure causes and mechanisms underlying these figures. Understanding these is, however, a crucial prerequisite in order to develop remedial measures. The failure modes, causes and mechanisms in converters in general and in wind-turbine converters in particular have therefore been chosen as main focus of the literature study summarised in the following.

It has been found that the wind-power specific literature dealing with converter failure is sparse. But in order to obtain an understanding of the potential failure modes and failure mechanisms, also literature not being limited to wind-power applications is considered a valuable source of information, even if e.g. the power cycling of subassemblies such as the power semiconductors is different in wind turbines compared to other applications. The following review will therefore use the available information on general reliability issues in power-electronic systems as a starting point.

2.1 Affected components of converter systems

Statistical information concerning the subassemblies or components in a converter system that are most frequently giving rise to a failure is provided in [17] and [18]. Figure 10 shows the results obtained by Wolfgang et al. [17] in a survey based on 200 products from 80 companies. According to this, the capacitors are identified as the most fragile components in converter systems, being followed by printed circuit boards (PCB) and the power semiconductors. In the second survey, which is based on 56 questionnaire responses from the power-electronics industry, Yang et al. [18] identify the power devices to be the most fragile part of the converter systems, see Fig. 10. Ranking second and third, also the capacitors and gate drives are identified as susceptible components.

The only wind-power specific information regarding the weak points in converters has been found in [19]: According to these authors (having a wind-turbine manufacturer background), the components with the highest failure rates in the converter are the IGBT-modules, the CCU-card (converter control unit) and the main fans. The failure rates of both the IGBT-modules and the CCU-card are stated to be strongly related to thermal cycling.

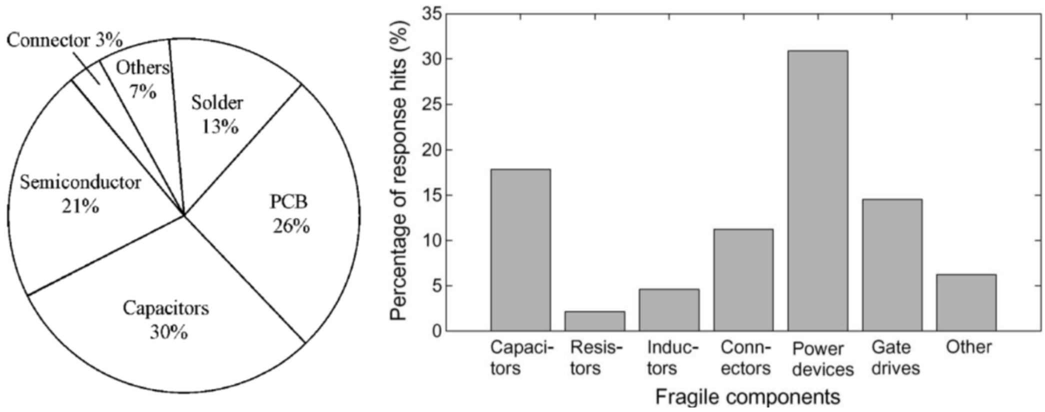

Fig. 10: Most fragile components of converter systems according to industry surveys published in [17] (left) and [18] (right)

2.2 Failure causes and mechanisms

A comprehensive review of the failure mechanisms and of condition-monitoring approaches for power-electronic converters is found in [20]. In the following, an overview over the identified chip-related and package-related failure mechanisms is given. It is mainly based on the abovementioned article, but complemented with information from additional sources and expert discussions as indicated.

Chip-related failure mechanisms

a) Electrical overstress

b) Latch-up and triggering of parasitic structures

c) Charge effects, ionic contamination or hot carrier injection

d) Electro-migration, contact- and stress-induced migration

e) Thermal activation

f) False triggering due to cosmic radiation

Package-related failure mechanisms

As mentioned earlier, it is necessary to distinguish between press-pack and module packaging technology. The following overview is limited to reliability issues of power modules, as these are the type of interest in the present work:

a) bond-wire lift-off

b) solder fatigue

c) degradation of thermal grease [10]

d) fretting corrosion at pressure contacts [21, 23]

e) tin whiskers [21, 22]

Bond-wire lift-off from both IGBTs and freewheeling diodes is regarded as one of the two principal failure mechanisms in power-electronic modules. It is caused by cumulative damage due to crack growth at the interface between the chip and the bond wire, resulting from temperature swings in combination with the difference in thermal-expansion coefficients (CTE) of Si and Al, see Fig. 11.

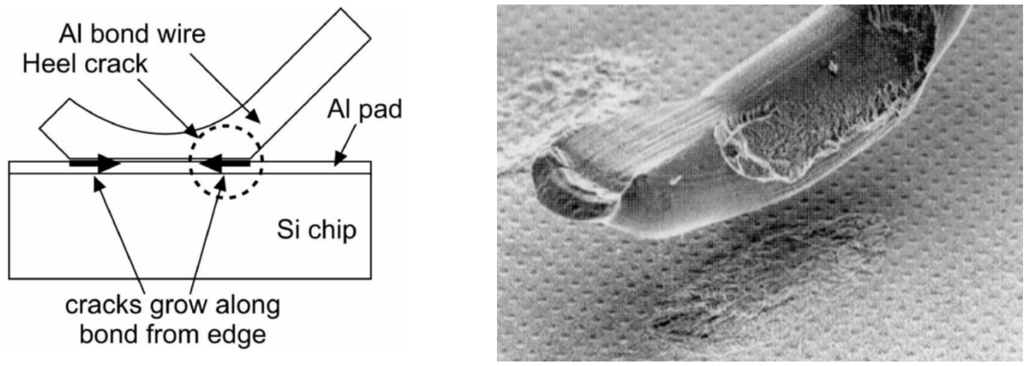

Fig. 11: Bond-wire lift-off due to crack growth: Crack propagation along the bond-wire/chip interface (left, [20]), SEM image of a lifted bond wire (right, [24])

Solder fatigue is considered the second principal failure mechanism in power-electronic modules. Again due to the difference in TEC between the adjacent materials being subject to thermal cycles, the solder cracks. Often starting from the edges off the solder area, the crack propagation leads to an increasing delamination. As a result, the heat-conducting area decreases, the thermal resistance between the chip and the heat sink increases and the chip fails due to overheating. Figure 12 illustrates the cracking and formation of voids due to solder fatigue.

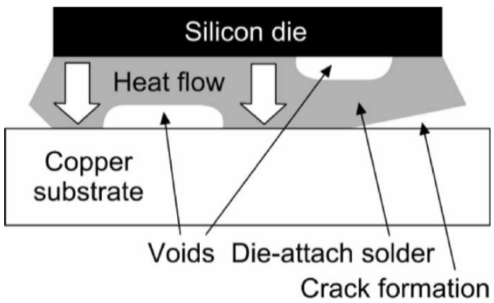

Fig. 12: Cracking and void formation due to solder fatigue [25]

The deterioration of the thermal grease connecting either the DCB or the base plate with the heat sink (see Section 1.2) leads to overheating of the power-electronic chips in a similar way as described above. The thermal grease usually consists of carrier oil mixed with ceramic powder or silicon-particles [26]. Subject to aging, this mixture tends to dry and turn into powder, which makes it a reliability-critical part of systems containing it [10].

Fretting corrosion is a form of accelerated atmospheric oxidation, which occurs at the interface of contacting materials undergoing slight, cyclic relative motion. In electric contacts involving non-noble metals, fretting action can cause rapid increases in contact resistance, proceeding to virtual open circuits within minutes in the worst cases. Fretting corrosion can be initiated by vibration or differential thermal expansion causing cyclic micro-scale relative motion in a contact interface. [21]

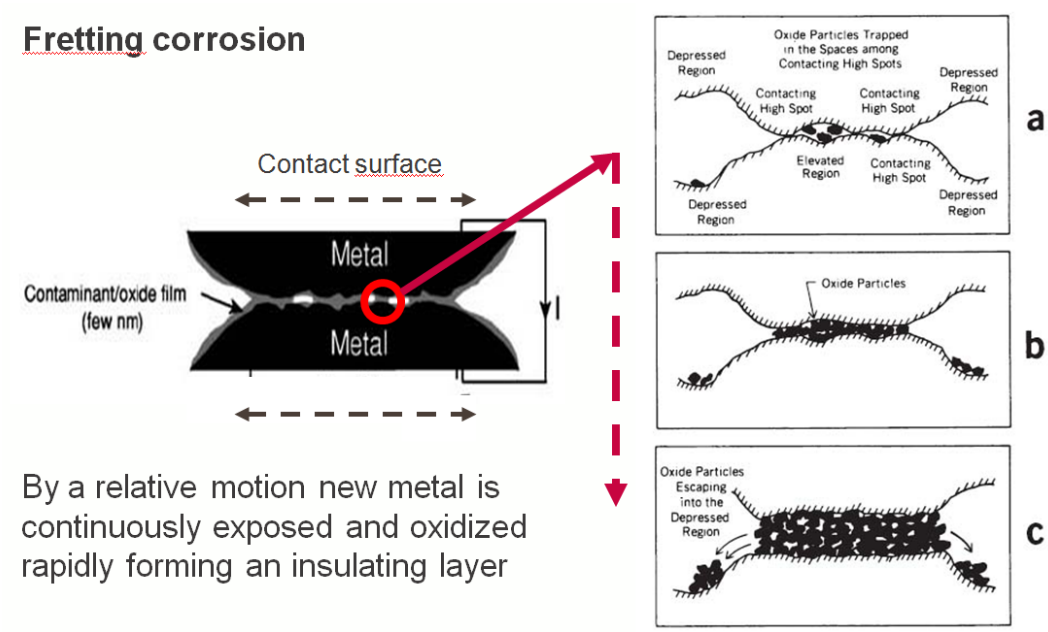

Fig. 13: Fretting corrosion at contact surfaces forming an insulating layer [21, 22]

The formation of tin whiskers, also called metal whiskering, is a phenomenon observed in electronic equipment produced using pure or almost pure tin solder. It describes the growth of micro-scale metallic hairs from tin solder pads, see Fig. 14. Whiskers can be a root-cause of short-circuit failure. The mechanism of whisker growth appears to be related to compressive mechanical stress. The addition of lead to the solder material effectively prevents the growth of whiskers, but its use has been restricted by the European Union in the early 21st century due to environmental and health issues afflicted with it. This gives rise to a re-emergence of the problem. In spite of their thin diameter not exceeding a few µm, tin whiskers can reach a length of several mm. Whiskers have been found to even poke through conformal coatings of circuit boards. [27, 28, 21]

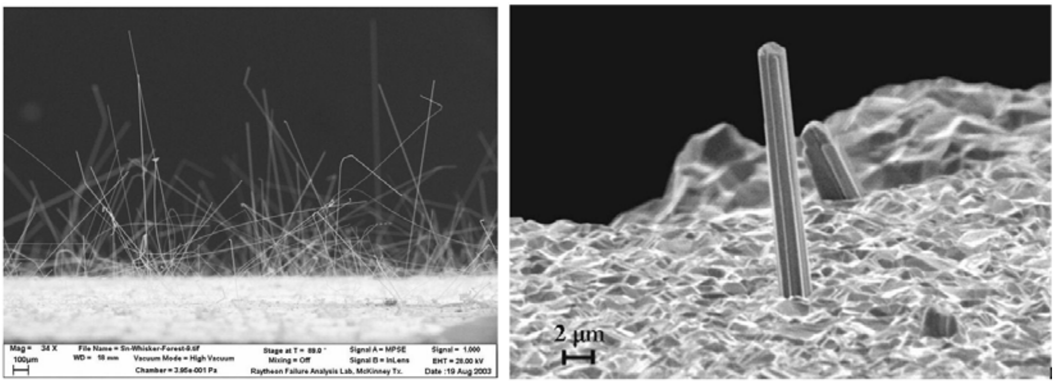

Fig. 14: Tin whiskers growing from tin solder pads, often giving rise to short-circuit failure [28]

2.3 Lifetime-relevant factors

It can be concluded from the previous section that packaging-related failure is often related to a thermal mismatch of the different materials in the module. Figure 15 shows the TEC of common materials used in power modules and illustrates the considerably higher expansion coefficient of Al and Cu compared to the other materials.

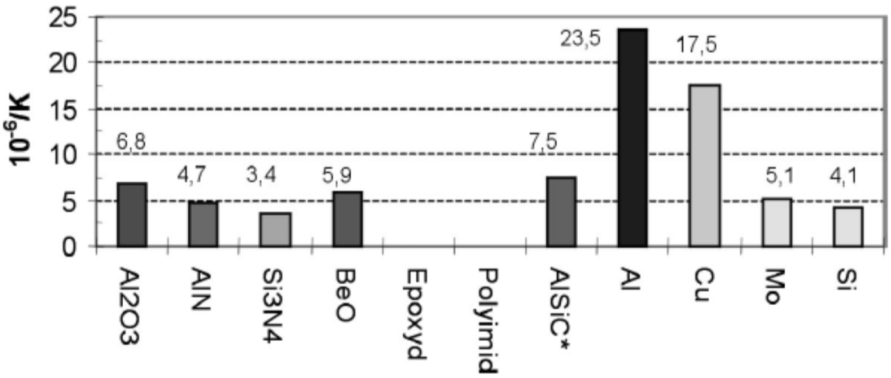

Fig. 15: Thermal expansion coefficients (TEC) of materials used in power modules [29]

Due to the central impact of the temperature swings ΔT on module lifetime, the manufacturers usually provide information about the power-cycling capability of their IGBT-modules. Figure 16 shows a typical power-cycling lifetime plot for industrial standard IGBT modules.

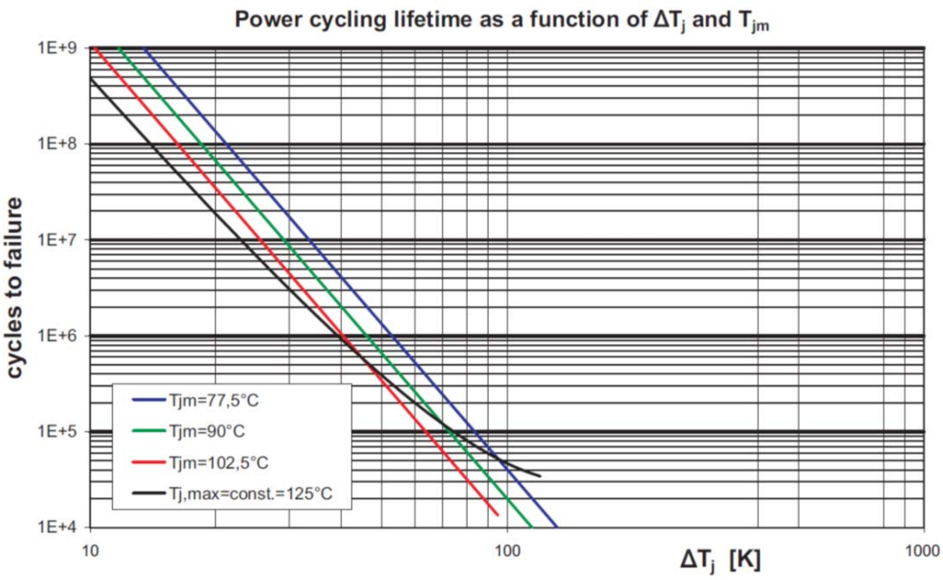

Fig. 16: Power cycling lifetime plot of standard industrial IGBT modules [11]

As also visible in the plot, the cycling lifetime is a function of the mean temperature during cycling as well as the amplitude of the junction-temperature swings ΔT. In addition, tests have indicated that further parameters such as the pulse duration t_{on}, the current amplitude I_B as well as packaging parameters like the bond-wire thickness, the bond-wire inclination angle, the chip thickness and the solder thickness have an impact on the power-cycling life-time. An extended empirical lifetime model including these factors, which is based on the analysis of a large number of tests, has been developed by Bayerer et al. [30]. It describes the number of power cycles to failure by means of the equation:

$$N_f = A \cdot \Delta T_j^{\beta_1} \cdot \exp\left(\frac{\beta_2}{(T_{j,min} + 273)}\right) \cdot t_{on}^{\beta_3} \cdot I_B^{\beta_4} \cdot V_C^{\beta_5} \cdot D^{\beta_6} \qquad (1)$$

The corresponding parameters, validity limits and coefficient values are given in Table 1.

Table 1: Parameters and limits for the lifetime calculation using Eq. (1) [30]

Parameters	Symbol	Unit	Limits	Coefficient	Value	Comment
Technology Factor	A				2.03E+14	Standard
Technology Factor	A				9.34E+14	IGBT4
Temperature difference	ΔT	K	45…150	β1	-4.416	
Min. chip temperature	$T_{j(min)}$	°C	20…120	β2	1285	
Pulse duration	t_{on}	s	1…15	β3	-0.463	
Current per bond foot	I_B	A	3…23	β4	-0.716	
Voltage class/100	V_C	V	6…33	β5	-0.761	
Bond wire diameter	D	µm	75…500	β6	-0.5	

2.4 Wind-power specific results

Wind-power and traction applications are considered to be among the most demanding application areas for power-electronic converters, see e.g. [20]. In wind turbines, the generator torque varies strongly with the wind speed, which in turn causes severely varying electrical and thus thermal loading of the converter.

In the available literature, results from two wind-power specific projects with a focus on converter reliability have been found: the work of Bartram and De Doncker at RWTH Aachen [26, 31] as well as the work of Fuchs and Mertens at Leibniz Universität Hannover [32]. Both projects focus on the reliability of IGBT converters in wind turbines with DFIG topology.

In the DFIG topology, the generator-side converter is stressed in a unique way: The DFIG rotor provides the converter with high electric current at low frequencies (0…<20 Hz). At frequencies approaching 0 Hz (synchronous operation of the DFIG), the junction-temperature cycles in the power-electronic chips are less and less damped by the thermal inertia of the system and therefore follow each sine-wave cycle of the DFIG rotor current. As shown in Fig. 17, this leads to thermal cycling with particularly high amplitudes. In addition, generator operation close to or at synchronous speed can cause a strongly asymmetric loading of the generator-side converter. [26]

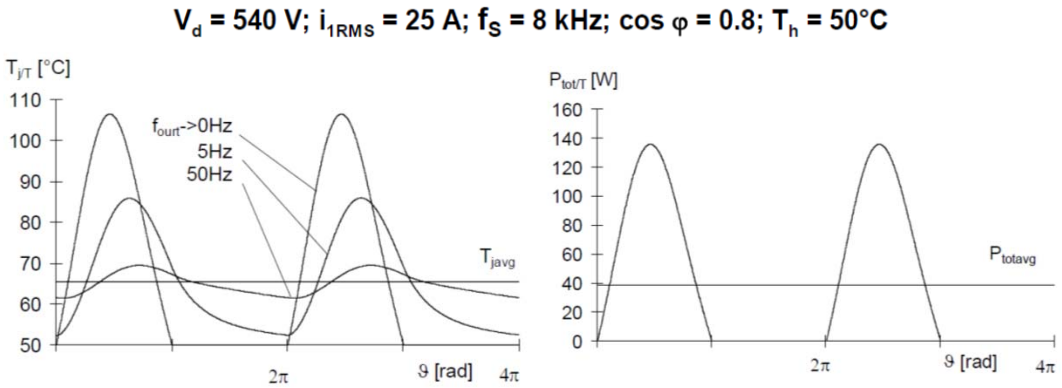

Fig. 17: Simulated junction temperature and power dissipation characteristics of a 1200V/50A-IGBT in inverter operation for different fundamental output frequencies [33]

In order to investigate the impact of low-frequency operation on the generator-side converter modules, Bartram carried out long-term power cycling tests at load-current frequencies of 0.4 Hz under lab conditions. Forensic analysis was carried out on modules which had failed during these tests as well as in the field. A junction-temperature swing of ΔT = 34 K was observed in the test setup.

The main findings in this work are (see also [26]):

- The IGBT chips appeared to be considerably more reliable than other parts in the module.
- Defect driver boards were the cause of several IGBT-module failures in the lab.
- A degradation of the thermal grease was observed in all investigated IGBT modules: thermal grease had been fluidized and squeezed out of the contact area. The grease was coloured black by particles originating from abrasion wear between the heat sink and the base plate or DCB, respectively. The remaining thermal grease had dried in large parts of the contact areas.
- Bond-wire lift-off and bond-wire damage has been observed, at ΔT as low as approx. 35K. The emitter bond-wires were found to have lower reliability than the gate bonds. This was explained by the fact that the emitter bonds lead the high load current, which causes Joule heating and thus an increase in bond-wire length. As a result, both shear and normal forces act in the interface area of the bond-wire and the chip. In contrary, the gate bond does not experience this as it carries virtually no current. Consequently only shear forces (resulting from TEC differences) act in the interface area. By means of forensic analysis of the damage patterns at the wire-chip interface areas, the abovementioned directions of forces acting in the contact areas of emitter / gate bonds with the IGBT could be confirmed.
- "Explosion", i.e. a complete destruction of the IGBTs including a shock-wave caused burst of the casing, was found to be a typical failure event resulting from a fault arc. In single cases, it could be shown that bond-wire lift-off had occurred on an IGBT chip before the destruction event.
- Solder damage was not observed, neither between the ceramic substrate and the base plate, nor between the IGBT chips and the ceramic. This was stated to be in agreement with the expectation that no solder fatigue would occur at thermal cycles with ΔT≤40 K.
- In the field, the protection provided by the converter cabinets was found insufficient: dust and even flies were discovered on the driver boards, the later ones attracted by silicone gel surrounding the IGBT chips. A thereby reduced creepage distance lead to spark-over between the IGBT collector and the gate, destroying the chip. Dust deposited on the driver board did not lead to spark-over in dry air, while already the presence of a low amount of humidity facilitated this effect.
- Two design improvements for driver boards were implemented together with a manufacturer to overcome the problem above: (a) lacquer coating of the driver board, and (b) additional slots in the driver-board in order to cut the creepage paths close to the connectors.
- The switch-off routines of wind turbines in the field were found insufficient in case of converter failure. As the authors state, destroyed IGBTs could be fed with several thousand Ampere before the turbine was disconnected from the grid.

The more recent (and in the instant of writing still on-going) work of Fuchs and Mertens presented in [32] focusses on the generator-side converter of a wind turbine with DFIG. Due to the earlier described mechanisms of high currents at low frequencies leading to severe thermal cycling, only the generator-side converter is considered lifetime critical.

For a 2 MW turbine and two example power-modules, electro-thermal simulation models are used to calculate the electrical behaviour and the junction-temperature swing over the whole wind-speed range between cut-in and cut-out speed. The model is based on the simplifying assumption that the turbine operates in steady-state at all times, i.e. that the tip-speed ratio is kept at its optimum value and the generator speed is only a function of the present wind speed. Using cycles-to-failure statistics and wind data from an offshore site from the year 2009, the lifetime-consumption of this year and its distribution over the wind-speed range is estimated.

Figure 18 shows the electrical characteristics of the investigated DFIG system, which provide a compact overview over the (steady-state) operating regime of the generator-side converter in a DFIG turbine. Figure 19 shows the corresponding junction temperatures of IGBTs and diodes vs. wind speed for a slim-dimensioned ("low-rated") and a generously-dimensioned ("high-rated") power module. Finally, Fig. 20 shows the resulting lifetime consumption for the two power modules.

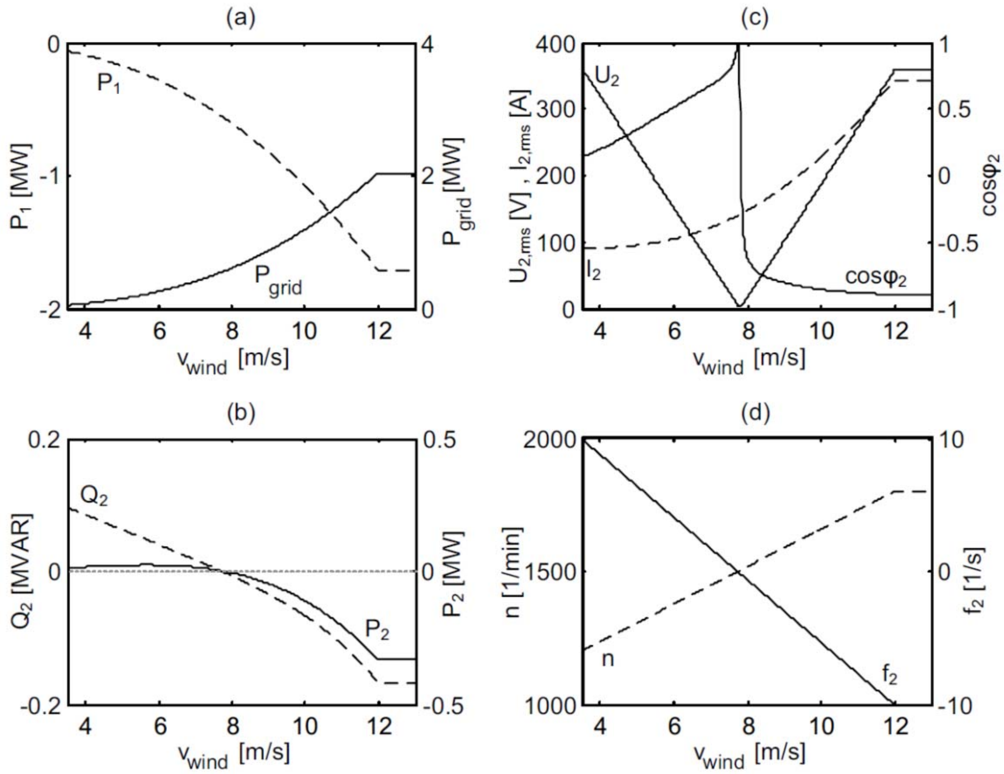

Fig. 18: Electrical operating behaviour in steady-state as a function of wind speed: (a) stator active power and total grid power, (b) rotor active and reactive power, (c) rotor voltage, current and power factor, (d) generator speed and rotor frequency ($v_{wind,cut-in}$=3.5 m/s; $v_{wind,sync}$=7.75 m/s, $v_{wind,rated}$=12 m/s) [32]

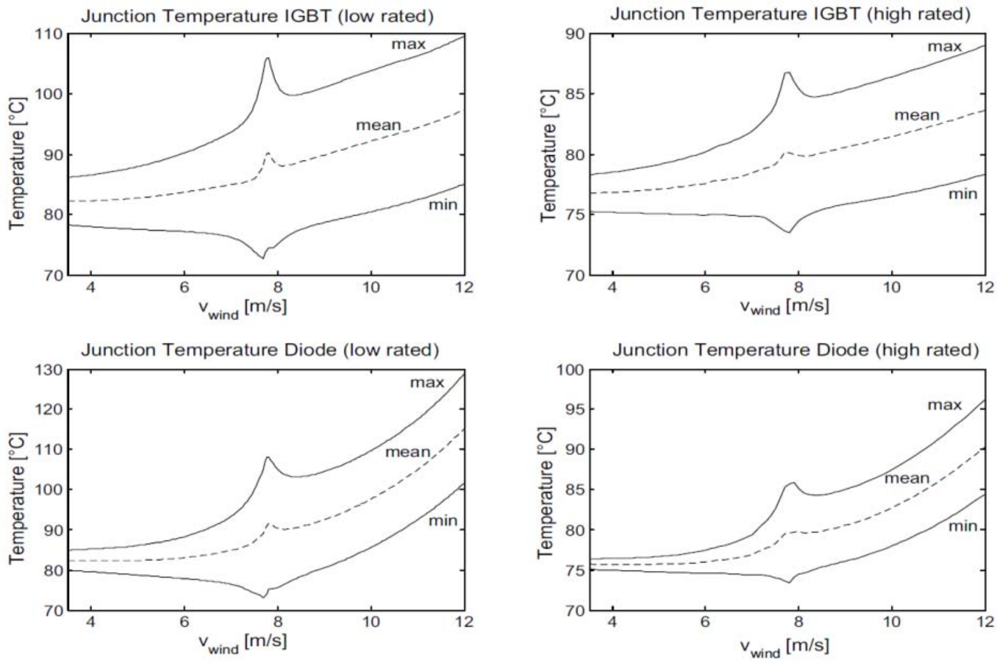

Fig. 19: Junction temperature of IGBT (top) and diode (bottom) over wind speed, for a low-rated (left) and a high-rated (right) power module [32]

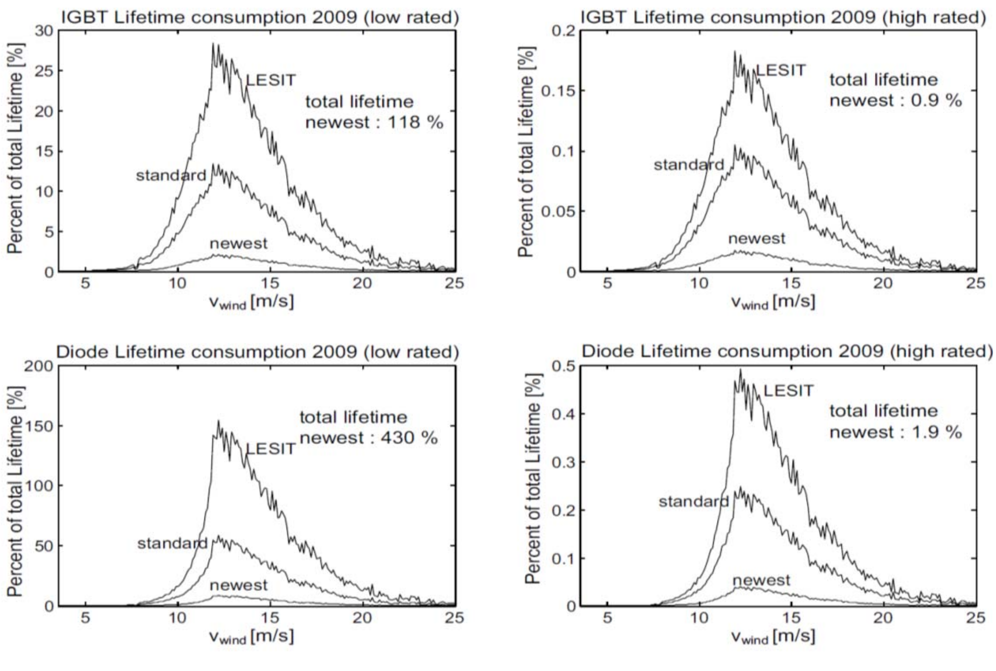

Fig. 20: Lifetime consumption of IGBT (top) and diode (bottom), for a low-rated (left) and a high-rated (right) power module, using different cycles-to-failure statistics [32]

The main findings and conclusions of Fuchs and Mertens [32] are:

- The highest lifetime consumption does not occur in or very close to the synchronous operating point (v_{wind} = 7.75 m/s), but at rated speed where the frequency is still <10 Hz and the current reaches the full rated current, see Fig. 18. According to these results, the operation at or close to synchronous speed is not critical.
- Among the power-electronic chips, the calculations suggest that the diodes are the lifetime-limiting components in the investigated system. This is due to a higher average temperature and a more severe temperature cycling in the prevailing over-synchronous operation, see also Fig. 19.
- The lifetime consumption differs significantly with the dimensioning of the modules. As Fig. 20 reveals, the expected lifetime of the high-rated module (Fig. 20, right) of ca. 50 years is substantially higher than that of the low-rated module (Fig. 20, left). This makes clear that the lifetime of IGBT converter modules must always be seen in connection with their dimensioning.

An extension of the present model to include dynamic operation of the system is subject of future work at Leibniz Universität Hannover.

In addition to the above reviewed experimental and model-based works on converter reliability in DFIG systems, Xie et al. [34] present a reliability model of a full-power converter system in a 2 MW wind turbine with permanent-magnet synchronous generator (PMSG). The converter system is modelled as a (reliability-wise) serial system consisting of generator-side converter, dc-link, grid-side inverter, filter and control system. Based on this structure and power-loss based estimations of the component temperatures at different operating points, an advanced failure-rate model is presented, which includes the effects of wind speed on converter reliability.

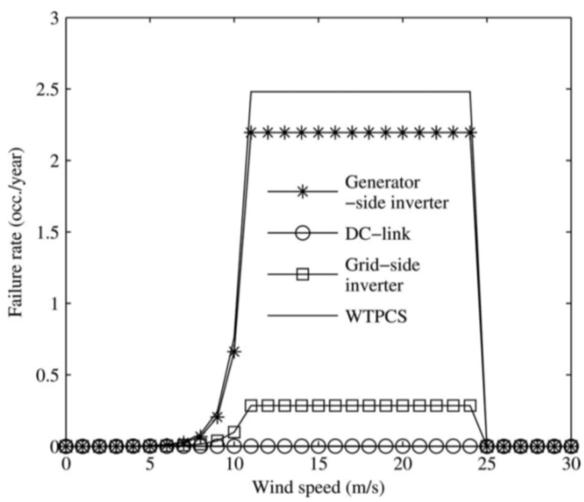

Fig. 21: Impact of wind speed on converter failure rates as proposed in [34]

The model results, shown in Fig. 21, suggest that the failure rate is highest at rated power. However, a key assumption in this work is that the heat-sink temperature and therefore the chip and driver-board temperatures are linear functions of the power losses. It means that the component temperatures are estimated highest at rated power, which is not generally the case for water-cooled modules. This limits the validity of the presented results and the relevance for this project with focus on water-cooled converter systems.

Interestingly also in this work dealing with a full-power converter in PMSG topology, the generator-side converter (in this case operating in a frequency range of 0…100 Hz) is stated to be the least-reliable component in the converter system.

3 Investigated systems

In the project described here, the analysis has been concentrated on two specific wind-turbine models with their respective converter systems. These will be referred to as:

(1) Wind turbine WT1

(2) Wind turbine WT2

A short introduction to the topology and relevant properties of the investigated turbine models is given in the following.

3.1 Wind turbine WT1

The turbine referred to as WT1 is equipped with a 4-pole doubly-fed induction generator (DFIG) with wound rotor. As shown in Fig. 1c, the generator stator is connected to the 690 V side of the transformer and therefore directly coupled to the electric power grid. The partially rated converter controlling the rotor current is connected to the 480 V output of the transformer. The converter consists of three modules on the generator side and three modules on the grid side see Fig. 22. Each module consists of hard-connected, paralleled half-bridges, which are controlled by a single gate-driver board. The structure of the converter system in WT1 is identical with the structure shown in Fig. 6, i.e. it contains 4-fold modules on the generator side and 3-fold modules on the grid side. All modules are water cooled.

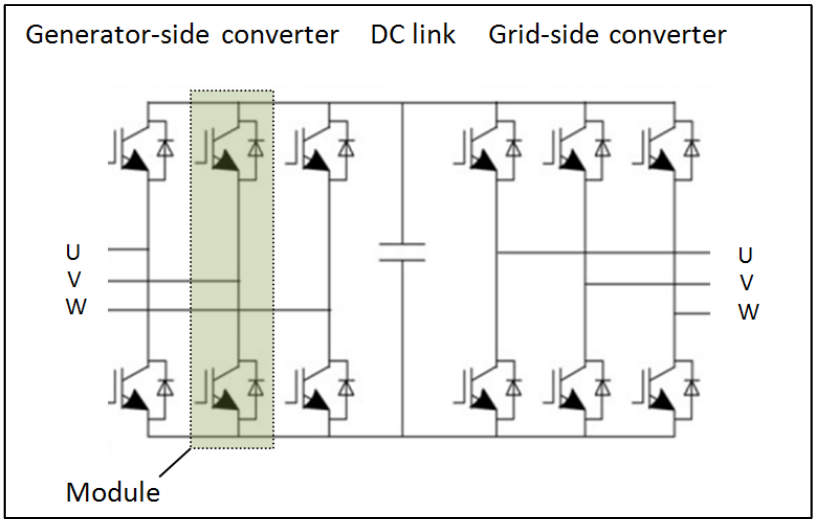

Fig. 22: Structure of the partially rated converter in turbine WT1

Fault-ride through capability is provided by means of DC choppers connected to the DC link (not shown in Fig. 22), which dissipate the excess energy in a controlled way through resistor banks in case of an increase in the DC link voltage.

In the WT1 system, the converter is located in the nacelle. For both the generator and the converter, the protection class describing the degree of (mechanical) protection against the environment is IP54.

3.2 Wind turbine WT2

The generator in the wind turbine referred to as WT2 is a fully-enclosed asynchronous machine with squirrel-cage rotor. Its stator is connected to the 690 V side of the transformer through a full-scale power converter, see also Fig. 1d. The converter allows generator operation at variable speed, frequency and voltage while it supplies power at constant frequency and voltage to the transformer. The converter system provides fault ride-through capability.
The structure of the converter in WT2 turbines is illustrated in Fig. 23.

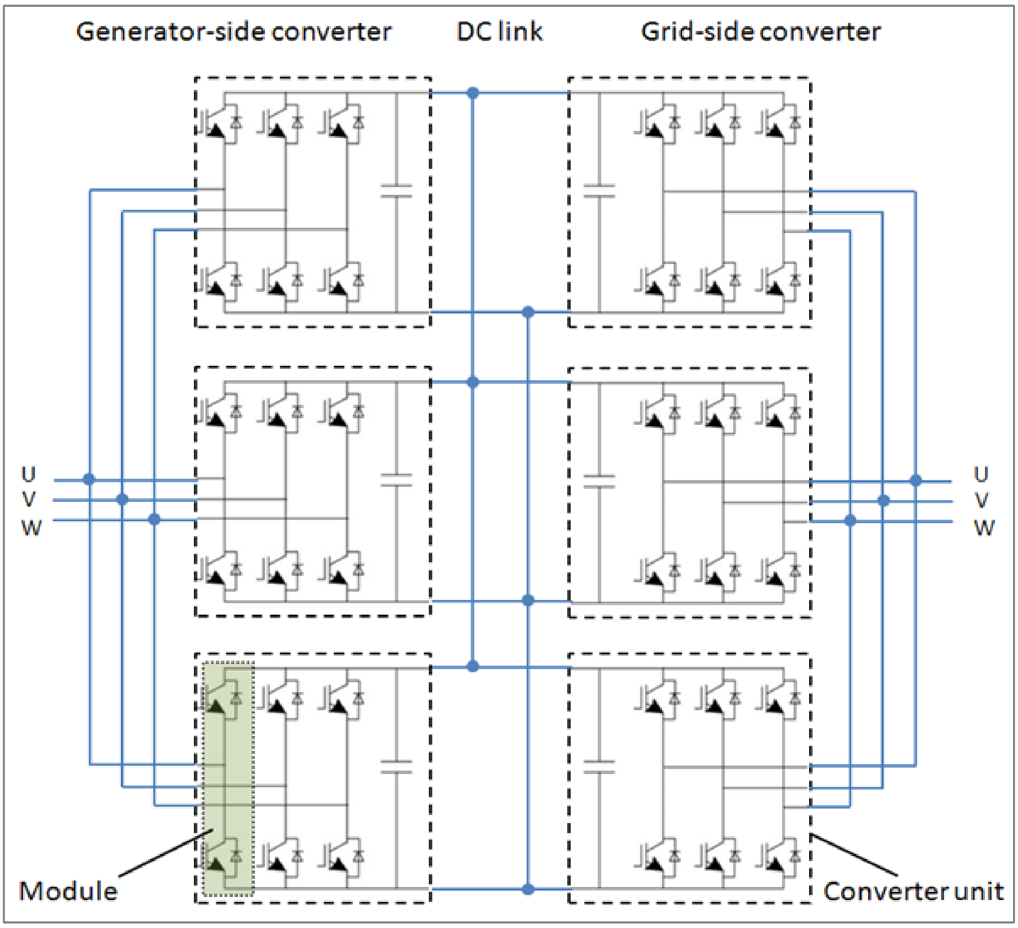

Fig. 23: Structure of the full-scale power converter in WT2, consisting of six units, each containing three converter modules

Both the generator-side and the grid-side converter consist of three units, each of which contains three 4-fold modules. Therewith, the converter consists of a total number of 18 modules. As shown in Fig. 23, the units are hard-connected in parallel both on the AC and the DC side. The current sharing between the paralleled units is monitored by the control system, which stops the turbine when the current unbalance between the units exceeds a predefined threshold value. The water-cooled modules used in the converter of WT2 are of a similar type as the ones applied in WT1.
However, unlike the case of turbine WT1, the converter of WT2 is located at the bottom of the tower.

4 Methods of analysis

With the objective to contribute to the clarification of the failure modes and causes of converter failure in wind turbines in the best possible way, a multi-track approach has been used in the present project, see also Fig. 24: In addition to the literature study presented in Chapter 2, a large amount of available data has been analysed, additional data has been collected at selected sites, and converter hardware has been tested and subjected to forensic analysis. The results of these different tracks have been used as input for two comprehensive Root-Cause Analysis meetings held with the expert group associated to this project.

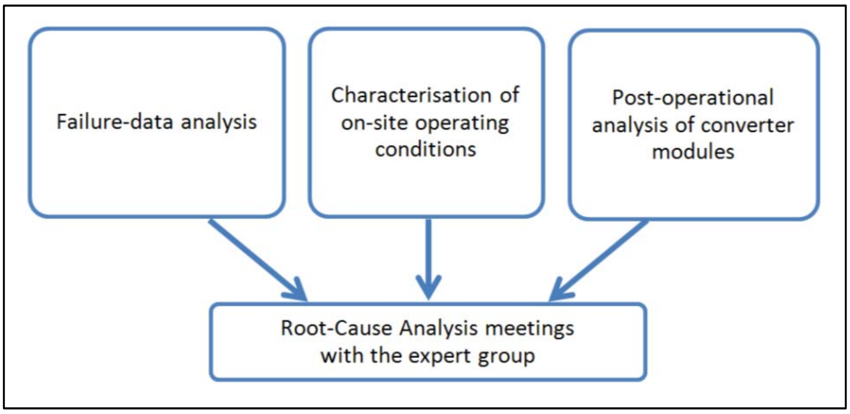

Fig. 24: Approach to the problem

The three analysis tracks shown in Fig. 24 are explained in more detail in the following.

4.1 Failure-data analysis

Failure and alarm data from both onshore and offshore sites with the turbine models of interest have been used in the project. Table 2 gives an overview over the wind parks from which data has been provided for the project. Note that the amount and type of data available for the sites in Table 2 varies significantly.

The main focus in the project has been set on the two offshore sites, Site A and Site D, for which the most comprehensive data has been available.

Table 2: Overview over wind parks from which data has been used in the project

Wind park	Turbine model	Site	Number of turbines
Site A	WT1	Offshore	>10
Site B	WT1	Onshore	≤10
Site C	WT1, WT1*	Onshore	>10
Site D	WT2	Offshore	>10
Site E	WT2	Onshore	≤10
Site F	WT2	Onshore	>10
Site G	WT2	Onshore	≤10

The following data has been used in the present project:

- annual statistics of converter-related alarm events logged by the SCADA systems (available for the sites listed in Table 2 from 2009 to 2011), provided by Vattenfall
- selected SCADA signals in a temporal resolution of 10 min from Site A and Site D for the years 2009 and 2010, provided by Vattenfall
- converter failure events incl. the date of failure and the affected turbine, compiled by Vattenfall based on maintenance work orders (available from Site A for the period Jan. 2009-April 2011 and from Site D for Aug. 2008 – Febr. 2012)
- climate data: daily average values of the ambient temperature and the humidity at the sites A and Site D, daily number of lightning strikes at and close to Site D for the periods covered by the failure data above, provided by the Danish Meteorological Institute (DMI) and the Swedish Meteorological and Hydrological Institute (SMHI)

A common measure for assessing the reliability of a component, particularly in lack of information about the component age, is the average failure rate. This is defined as

$$f = \frac{\sum_{i=1}^{I} N_i}{\sum_{i=1}^{I} X_i \cdot T_i}, \qquad (2)$$

with N_i denoting the number of failures of the component in the time interval i, X_i describing the number of systems reporting to the database in time interval i, and T_i being the duration of the time interval i. Failure rates are usually given in failures per system and year.

In the present study, both average failure rates and alarm rates have been analysed in order to identify potential differences related to the turbine topology or the site being located onshore vs. offshore. With the objective to identify possibly age- or season-related changes in the converter reliability, the temporal evolution of the average annual and monthly failure rates has been analysed. Besides the consideration of temporal variations in the failure rates, also the spatial distribution of failures in the offshore parks Site A and Site D has been considered in order to reveal likely factors influencing the converter failure.

For the same two offshore sites, the available failure data has been analysed together with climate data in order to identify to which extent the environmental conditions ambient temperature, ambient humidity, wind speed and lightning strikes are correlated with converter failure.

For this purpose, a simple linear correlation analysis has been carried out:
The linear correlation coefficient, also called Pearson's correlation coefficient, quantifies the strength of a linear relationship between two variables X and Y. From a series of n measured pairs of X and Y, denoted x_i and y_i with i = 1,…,n, the Pearson correlation coefficient of the population can be estimated using:

$$r_{xy} = \frac{\sum_{i=1}^{n}(x_i - \bar{x})(y_i - \bar{y})}{(n-1)s_x s_y} = \frac{\sum_{i=1}^{n}(x_i - \bar{x})(y_i - \bar{y})}{\sqrt{\sum_{i=1}^{n}(x_i - \bar{x})^2 \sum_{i=1}^{n}(y_i - \bar{y})^2}} \tag{3}$$

Herein, $\bar{x}$ and $\bar{y}$ are the sample mean values of X and Y while s_x and s_y denote the sample standard deviations of X and Y.

In addition to the value of the correlation coefficient, a second quantity of interest is the p-value for testing the hypothesis of no correlation against the alternative that there is a non-zero correlation. Low values of p, e.g. $p<0.1$, indicate that the correlation between the two quantities X and Y is significantly different from zero.

In the present study, the linear correlation analysis has been applied to investigate the correlation between the number of converter failures in a park with the average environmental conditions during the same period. The analysis has been carried out on a monthly and, where possible, on a daily scale.
A correlation analysis on the daily scale requires knowledge about the exact date on which a converter failure initiated. By combining the failure data, providing the approximate date of failure and the affected turbine, with the alarms logged by the SCADA system of the same turbine, it was often possible to determine the date at which a converter problem started. In case

of an existing correlation between the failure and an environmental factor, it can be expected that the conditions being present at the initiation of the problem are those relevant for the failure.

4.2 Characterisation of the on-site operating conditions

A simple but crucial question in the context of failure analysis is if the real operating conditions of the component of interest in the field comply with the specifications this component has been designed for.
According to the literature study carried out within this project, little is known about the real on-site operating conditions of converters in wind turbines so far.
Due to this, an attempt has been made in the present study to characterise the operating conditions of the converters in the field, both with respect to their loading and to their operating environment inside the converter cabinets. While an estimate of the load profile can be obtained from the available 10-min SCADA data, additional data has been collected in the project to investigate the latter aspect.

By means of small battery-driven loggers of the type Lascar EL-USB-2 (see Fig. 25a), the temperature and the relative humidity inside the converter cabinets of several wind turbines has been recorded. The loggers were installed in the upper part of the cabinets and have recorded the indicated quantities over a period of several weeks during April-June 2012 with a sampling interval of 30 min.

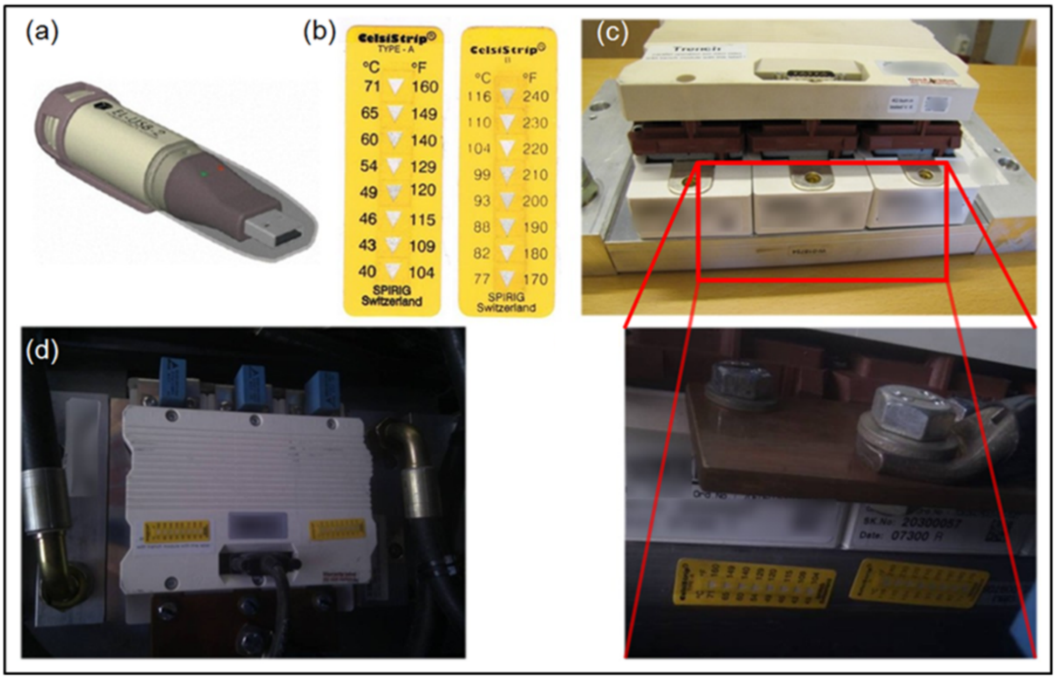

Fig. 25: Temperature and humidity loggers (a) and thermo-sensitive tape (b) applied for on-site measurements inside the converter cabinets; position of the thermal tape at the side of the module heat-sink (c) and on the module

top-cover (d); Source: Figure (a) from [35], Figures (c) and (d) by courtesy of Vattenfall

In order to collect information about the operating temperatures reached by the converter modules, THERMAX Irreversible Temperature Recording Strips have been used to indicate the local maximum temperatures on the heat sink and on the module cover, i.e. directly on top of the gate-driver boards (see Fig. 25b-d).

Table 3 gives an overview over the sites and turbines at which the converter operating conditions have been investigated in this way.

Table 3: Wind turbines equipped with temperature and humidity loggers

Wind park	Turbine model	Site	Number of turbines equipped with loggers
Site A	WT1	Offshore	2
Site B	WT1	Onshore	2
Site D	WT2	Offshore	2
Site E	WT2	Onshore	1

Finally, it has been possible to collect vibration data from a converter on a turbine at Site A. For that purpose, an acceleration sensor of type AS-062 has been mounted directly on the heat sink of one of the rotor-side converter modules and the vibration signal has been recorded at different loading conditions of the turbine using the existing condition-monitoring system. The location of the mounted acceleration sensor on the converter module is shown in Fig. 26.

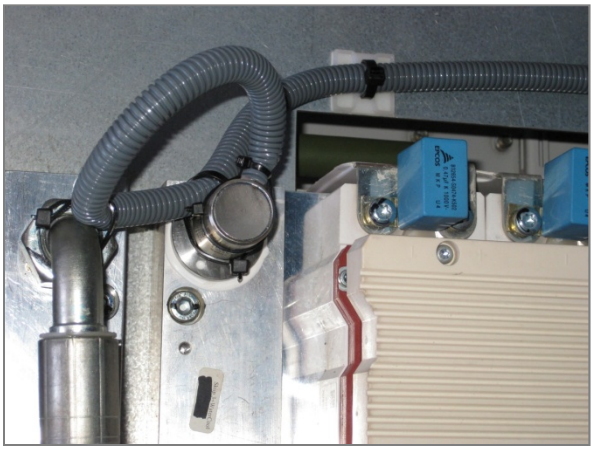

Fig. 26: Acceleration sensor mounted on a converter module, picture by courtesy of Vattenfall

4.3 Post-operational analysis of converter modules

In addition to the analysis of failure data and the characterisation of the converter operating conditions described above, it has been possible to investigate several replaced converter modules from Site A.

While no information about the operational age of these modules is available, their manufacturing dates are denoted directly on the modules. These range from 2006 to 2010, with the majority of modules being produced in 2006. The maximum operational age of the modules is therefore 6 years. Taking into account the year of commissioning of Site A, this indicates that none of the investigated modules belongs to the first generation of converter modules the turbines were delivered with, i.e. that at least one replacement of converter modules had occurred before in the respective wind turbines.

With the objective to identify the affected parts of the modules and to obtain indications for the mechanisms of failure, the available converter modules have been utilised in two different types of analyses:

Nine modules without visible signs of destruction have been subject to different electrical measurements using the DSUB connector to the gate-driver board as well as the AC and DC terminals. The tests have covered

- the measurement of the insulation resistances between different parts of the gate-driver board and the heat sink,
- the measurement of the withstand voltage,
- the measurement of the on-state forward voltage drop of the IGBTs and diodes,
- a functionality check of the IGBTs and diodes, and
- a functionality check of the module-internal temperature and current sensors.

Two converter modules with obvious signs of destruction were subject to forensic analysis. For this purpose, the modules were opened and inspected visually, by means of an optical microscope as well as, in one case, using a scanning electron microscope.
Additional converter modules without any visible signs of destruction were investigated at the external test laboratory Swerea IVF, Göteborg, with the objective to assess the integrity of the IGBT chip-solder and the bond wires in the modules. The latter analysis was carried out using visual/optical inspection with a stereo microscope, X-ray microscopy inspection, scanning acoustic microscopy (SAM) analysis and scanning electron microscopy / energy dispersive spectroscopy (SEM/EDS).

In order to ensure that all findings could be related to the field operation of the converter and had not possibly been introduced during the above described electrical measurements, different modules have been used for the two types of analysis.

5 Results and discussion

The presentation and discussion of the analysis results is structured in accordance with the three main analysis tracks introduced in the previous chapter. Unless it serves the purpose of comparison, separate sections are used for the results concerning the two investigated turbine models WT1 and WT2 to facilitate their distinction.

5.1 Failure-data analysis

According to a number of discussions preceding and during the project, there is a common perception that converter failure occurs more frequently in offshore than in onshore wind parks. As a first step, the converter-related failure and alarm data available for both onshore and offshore installations of the turbines of interest has therefore been analysed with the objective to find evidence in favour of or against this hypothesis. Table 4 provides a compilation of the average failure-event and alarm rates obtained for the different wind parks using Eq. (1), based on data ranging from 2009 to 2011.

Note that, here as well as in the following, a converter failure is considered a single failure event even if several converter modules are affected and might have been replaced sequentially throughout a period of some days.

Table 4: Converter-related average failure and alarm rates for the turbine models and sites of interest

Wind park	Turbine model	Site	Avg. failure event rate [1/turbine/yr]	Avg. failure event rate [1/module/yr]	Average alarm rate [1/turb./yr]
Site A	WT1	Offshore	0.13	0.020	0.9
Site B	WT1	Onshore	n.a.	n.a.	46.5
Site C	WT1 WT1*	Onshore	0.15	0.025	5.4
Site D	WT2	Offshore	0.39	0.021	6.1
Site E	WT2	Onshore	n.a.	n.a.	2.5
Site F	WT2	Onshore	n.a.	n.a.	2.0
Site G	WT2	Onshore	n.a.	n.a.	1.7

The failure-event rate obtained for turbine WT1 shows a good agreement between the offshore Site A and the onshore Site C. In contrary, it is considerably higher for the WT2 operating at Site D. Interestingly, a normalisation with the number of converter modules per turbine reveals a very similar average number of failures per module and year, in spite of the different turbine topologies of WT1 and WT2 (see Table 4).

The average alarm rate is found to differ considerably between the sites, even among turbines with identical SCADA systems. As a comparison of the cases of Site A and Site C shows, the alarm rate does not necessarily have a correlation with the failure rate. While the SCADA alarm data has been analysed in order to allow the inclusion of a larger number of sites in the comparison, it must be concluded that the rate of converter-related alarms does not appear to be a valid measure for converter reliability. It is therefore not used in the further analysis.

In summary, the available failure data does not confirm the abovementioned perception of converter failure occurring more frequently at offshore sites. A factor that might be suggestive of more severe converter problems at offshore sites is the usually much longer time to repair at these sites, due to accessibility constraints resulting from wind and waves. The related production loss makes the economic consequences of a converter failure offshore typically more severe than onshore.

5.1.1 Results for wind turbine WT1

Temporal distribution of converter failures

Based on failure data from Site A ranging from January 2009 to April 2011, the average annual failure rate and the distribution of failures over the months of the year has been determined, see Fig. 27.

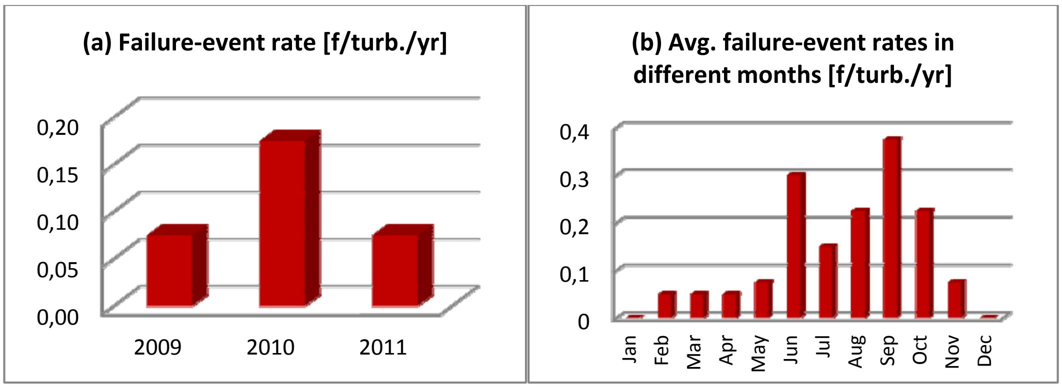

Fig. 27: Temporal distribution of converter failures at Site A during January 2009 - April 2011

While the period of observation is too short to observe possible age-related changes in the converter reliability, Fig. 27b reveals that the seasons summer and autumn are most critical with respect to converter failure at this site.

Spatial distribution of failures

An analysis of the spatial distribution of failures in a wind park has the potential to reveal the occurrence of repetitive failures on single wind turbines as well as possible failure patterns, e.g. a correlation with the prevailing wind direction.
For Site A, analysis of failure data from Jan. 2009 – Apr. 2011 reveals repetitive failure for a turbine located in the middle of the wind park. Otherwise, the failures are spread randomly over the wind park and do not show any pattern that would allow further conclusions.

Correlation with climatic factors and wind speed

In order to identify environmental factors being correlated with failure, converter failure data from Site A has been analysed in combination with climate data from a nearby measurement station and with wind-speed data recorded by the turbine SCADA systems. Figures 28a-d show the monthly number of converter failures together with the average values of the ambient temperature, the ambient relative humidity and the wind speed in the respective month. Not surprisingly, the average temperature is highest during the summer months, while the relative humidity reaches its maxima in the winter and wind speed reaches the highest average values in autumn.

In order to quantitatively assess the correlation between converter failure and the enviromental factors temperature, relative humidity and wind speed, linear correlation analysis as described in Section 4.1 has been applied to the monthly average values shown in Fig. 28. The resulting correlation coefficients and p-values are compiled in Table 5.

The only statistically significant correlation is found between converter failure and ambient temperature. Some negative correlation is observed with the relative humidity. However, as a failure rate decreasing with the relative humidity is physically not plausible, this should mainly be ascribed to the strong negative correlation of temperature and relative humidity. No statistically significant correlation is found between converter failure and the average wind speed.

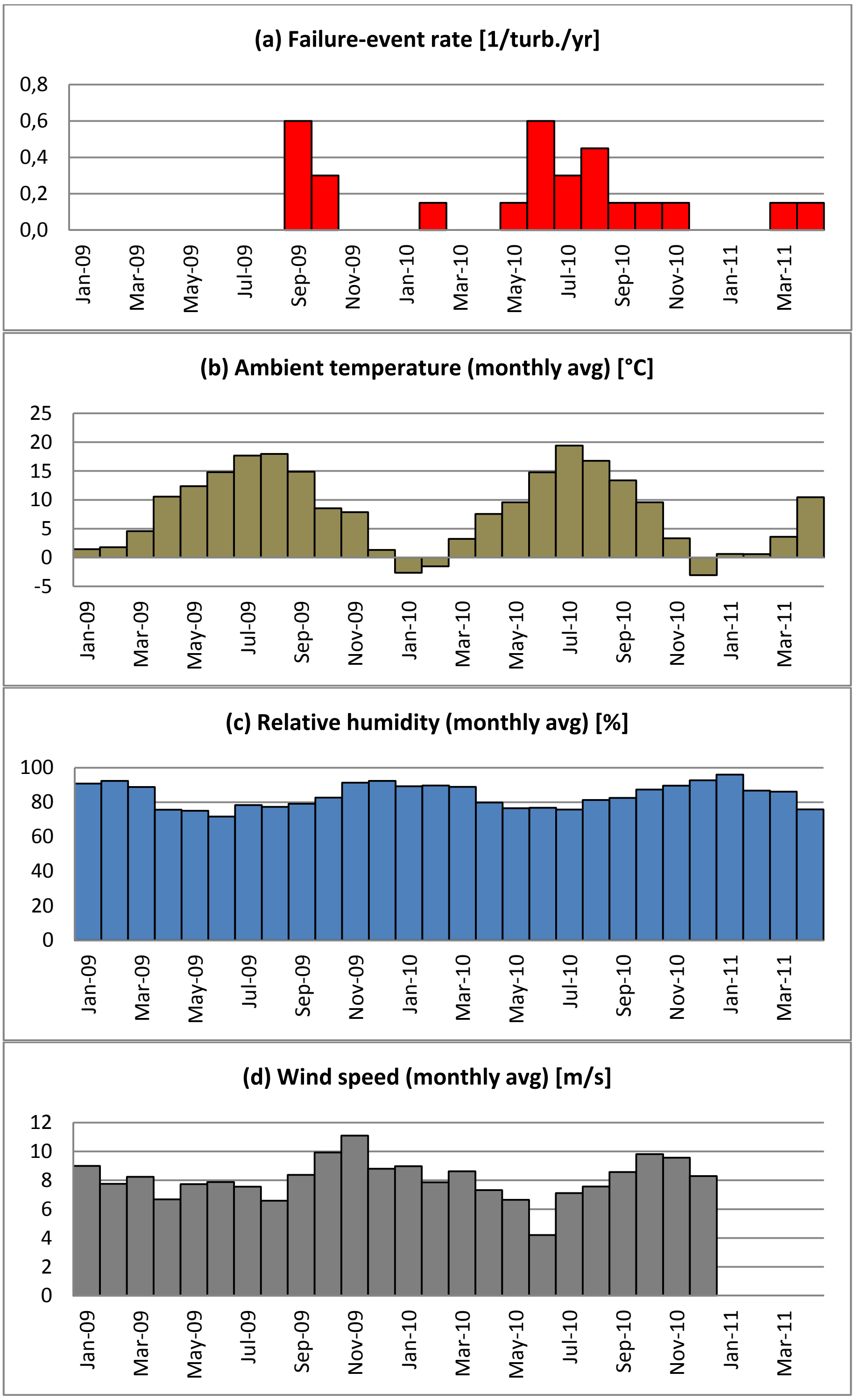

Fig. 28: Converter failures and monthly average values of ambient temperature, relative humidity and wind speed at Site A

Table 5: Correlation-analysis results obtained from monthly values of failure, temperature, relative humidity and wind speed

Environmental factor	Correlation with failure, using monthly avg. data
Average ambient temperature	r=0.46, p=0.014
Average relative humidity	r=-0.33, p=0.082
Average wind speed	r=-0.30, p=0.153

5.1.2 Results for wind turbine WT2

Temporal distribution of converter failures

Failure data from Site D ranging from August 2008 to February 2012 has been used to calculate the average annual failure rate and the distribution of failures over the months of the year for this wind park. These are shown in Fig. 29.

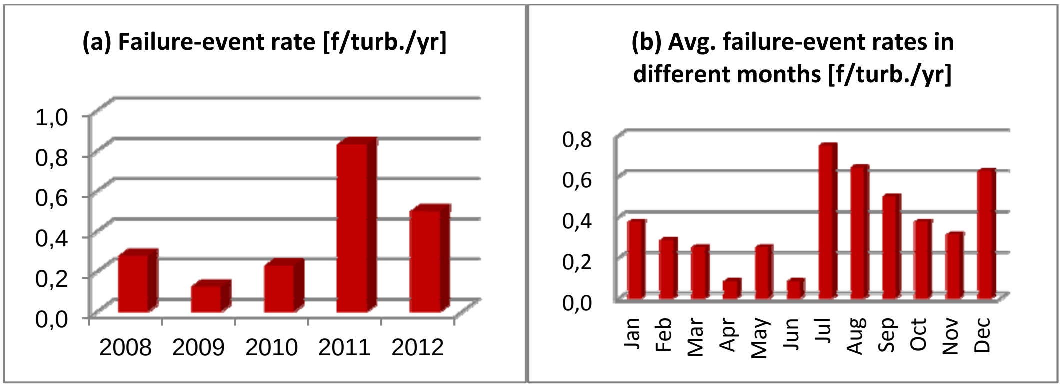

Fig. 29: Temporal distribution of converter failures at Site D during August 2008 - February 2012

As in the case of Site A, converter failure is observed most frequently during the seasons summer and autumn, see Fig. 29b. Figure 29a suggests a systematic, possibly age-related increase in the failure rate. (Note that due to the unequal distribution of failure events over the course of the year, the failure rate calculated for 2008 based on only the last five months of the year might be higher than the real average value for 2008, while the failure rate estimated for 2012 based on the two first months of the year might underestimate the real value.)

Additional information available for Site D is the mode of converter failure. As shown in Fig. 30, these are clearly dominated by explosion failure and so-called sharing faults, both having approximately equal shares. Sharing faults imply a control-system induced shutdown of the turbine when an unbalanced current-sharing between the paralleled converter units in the WT2 is detected.

This is usually the case when a converter module fails to switch. However, it can also have module-external causes like loosened cable connections.

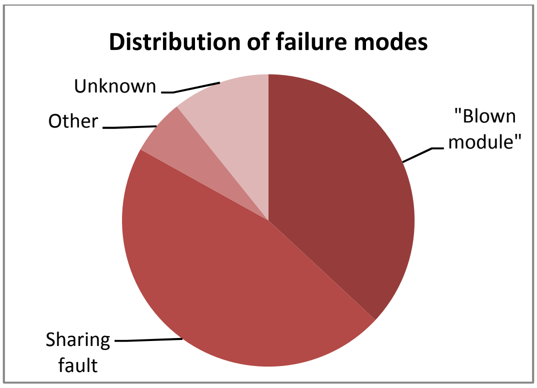

Fig. 30: Distribution of converter failure modes at Site D

Spatial distribution of failures

The spatial distribution of converter failure events at Site D during Aug. 2008 - Feb. 2012 has been analysed. The number of converter failure events per turbine during this period ranges from zero up to five failures.
In contrary to the results obtained for Site A, a concentration of failures is observed in the part of the park located towards the prevailing wind direction. At the same time, the most affected wind turbines are the ones being located closer to the ends of the radial grid-connection cables.

There are several possible explanations for the observed pattern:

- The rows of wind turbines being located towards the prevailing wind direction are typically those facing the strongest wind and therefore having the highest production. A higher electrical loading of wind turbines is likely to lead to an increased risk of converter failure.
- According to Eliasson and Isabegovic (2009), the wind turbines located at the end of the radial connection grid are subjected to the highest over-voltages. Another possible explanation for the concentration of converter failure at the radial ends is therefore that turbines in these locations experience the highest electrical stress in case of disturbances in the grid.
- A third possible explanation for the observed pattern is that thunderstorms will most likely move over the wind park in the prevailing wind direction and towards the coastline. In that case, it can be expected that the turbines in the most failure-affected part of the park are the ones being most frequently hit by lightning strikes.

Lightning impact
In order to further investigate the possible correlation of converter failure with lightning strikes, lightning data from the Site D and its surrounding area has been analysed together with the failure data.

A first comparison of the annual number of converter failures per turbine and lightning strikes in Fig. 31 reveals an interesting coincidence between these on the annual timescale. In particular, an extraordinarily high number of lightning strikes in 2011 coincides with a high number of converter failures in that year.

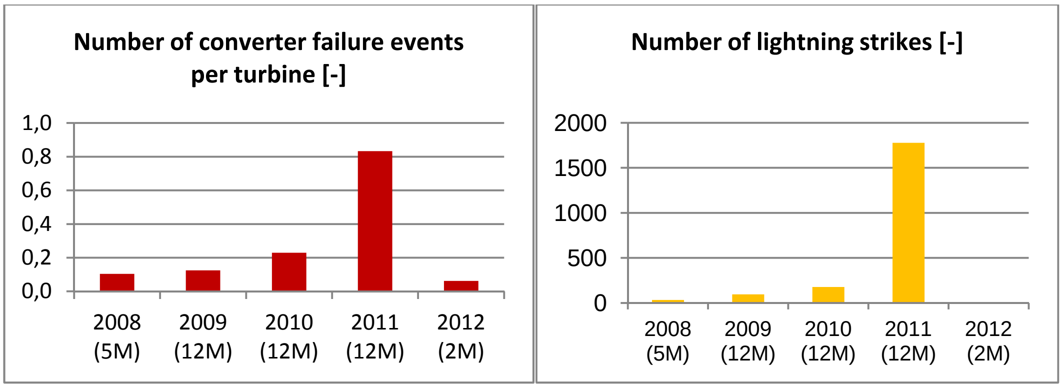

Fig. 31: Annual numbers of converter failures and lighting strikes at Site D

Figure 32 allows a visual comparison of the failure and lightning numbers on the monthly scale. This confirms a noticeable coincidence between the two phenomena. The apparent discrepancy observed for the period October – December 2011 can be explained by the fact that positive lightning strikes occur during the cold seasons, which are considerably stronger than negative strikes. The occurrence of a low number of strong lightning strikes during late 2011 could therefore still have contributed to the high number of converter failures during this time.

In order to quantitatively assess the correlation between converter failure and lightning strikes, linear correlation analysis has been applied to the monthly average values shown in Fig. 32. The resulting correlation coefficient of $r = 0.48$ with $p = 0.001$ confirms the visual impression of a strong correlation.
In addition to the analysis on a monthly scale, for the case of Site D, it has been possible to perform a correlation analysis even on the daily scale. As described in Section 4.1, this requires exact knowledge of the date on which a failure started. In the present case, the analysis was therefore based on the failure events occurred during Jan. 2009-Dec. 2011, excluding four events reported in the failure data, for which no indication could be found in the SCADA alarm logs.

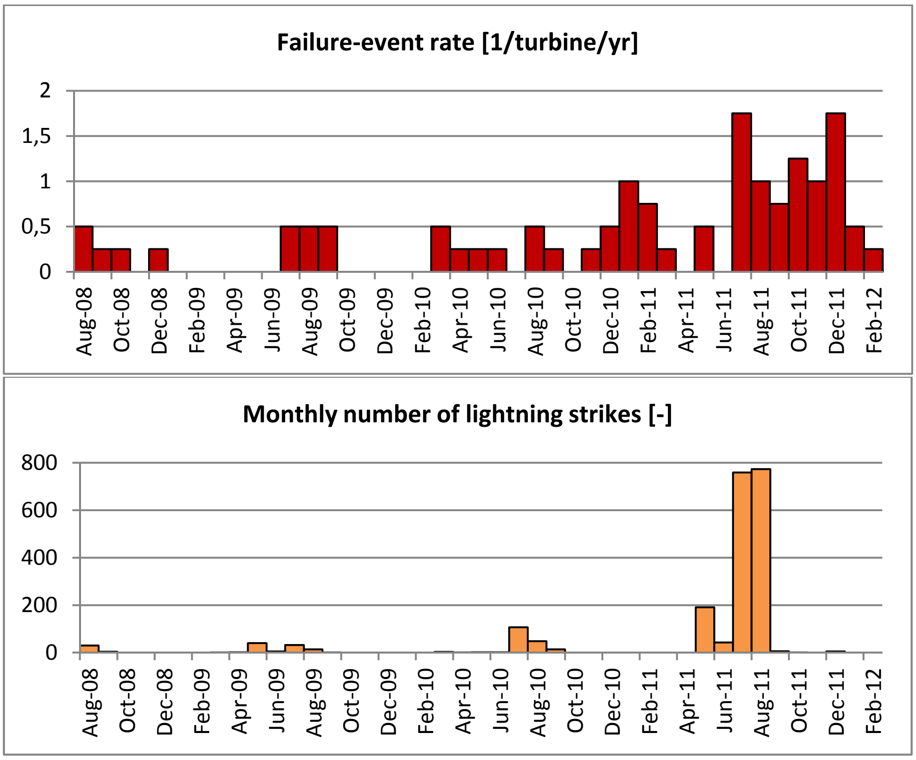

Fig. 32: Monthly converter failure and lightning strikes at Site D

Interestingly, the much more informative correlation analysis on the daily scale confirms a statistically significant correlation between the number of failures and the number of lightning strikes ($r = 0.11$, $p = 0.0002$). A particularly significant correlation is found between explosion failures and lightning strikes ($r = 0.15$, $p = 3 \cdot 10^{-7}$). This is a strong indication that lightning strikes are a relevant factor for converter failure and in particular for the failure mode of thermal destruction.

Among the possible ways in which lightning strikes can have an effect on wind turbines are the direct hit by a lightning strike, a rise in the ground potential or disturbances in the collection grid of the wind park.

Correlation with climatic factors and wind speed

In order to identify possible further environmental factors being correlated with failure, the converter failure data from Site D has been analysed in combination with climate data from a nearby measurement station and with wind-speed data recorded by the turbine SCADA systems. Figures 33a-d show the monthly number of converter failures together with the average values of the ambient temperature, the ambient relative humidity and the wind speed in the respective month.

As expected, the average temperature is highest during the summer months. Both the relative humidity and the wind speed reach their highest values during autumn and winter.

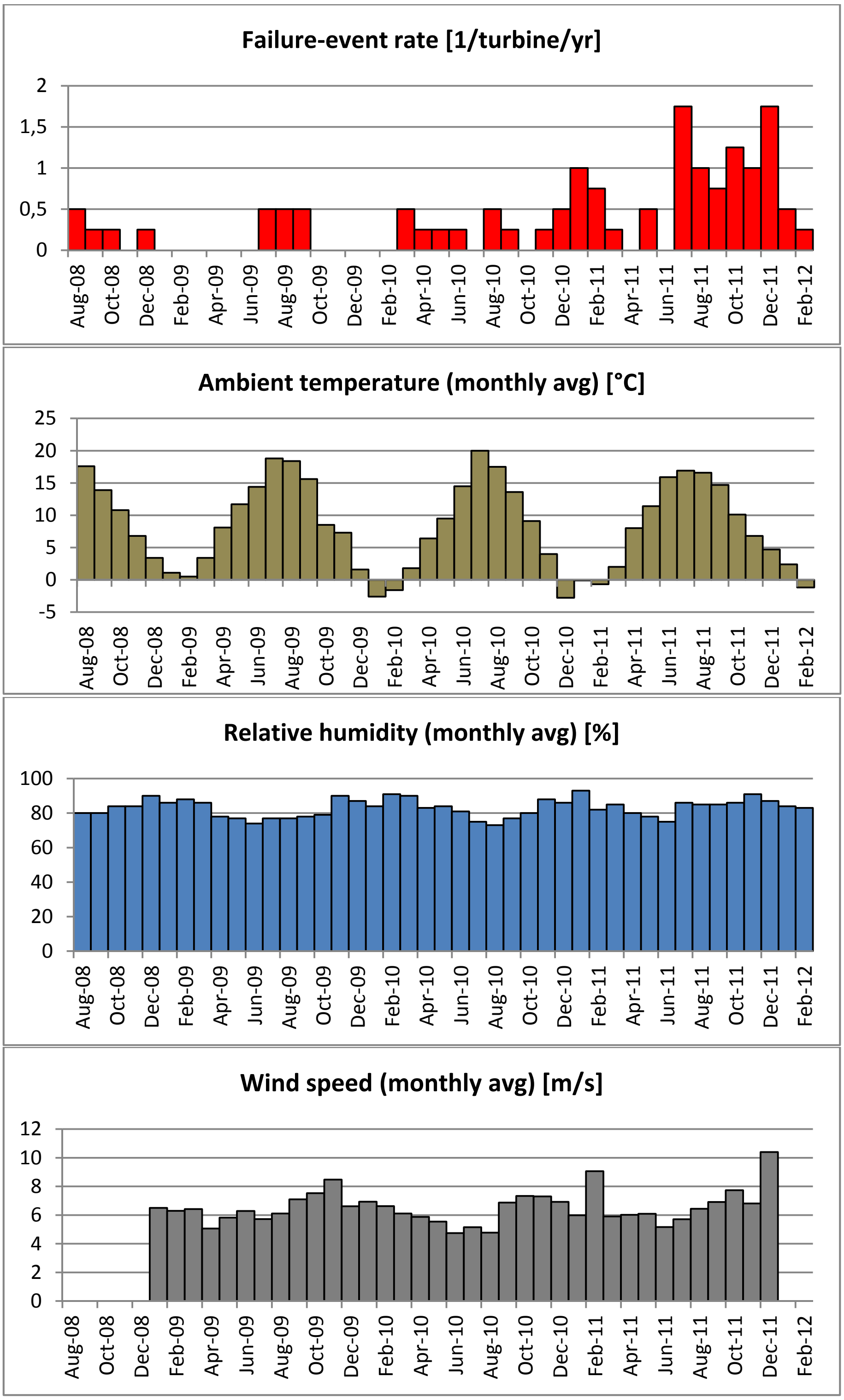

Fig. 33: Converter failures and monthly average values of ambient temperature, relative humidity and wind speed at Site D

Table 6 summarises the results of the linear correlation analysis, both using monthly and daily average values. While the first is based on the data shown in Fig. 33, the latter is limited to data from the period January 2009 - December 2011.

Table 6: Correlation-analysis results obtained from monthly and daily values of failure, temperature, relative humidity and wind speed for Site D

Environmental factor	Correlation with failure, using monthly avg. data	Correlation with failure, using daily average data
Avg. amb. temperature	r = 0.14, p = 0.36	r = 0.04, p = 0.15 (explosion: r = 0.03, p = 0.34)
Avg. relative humidity	r = 0.28, p = 0.07	r = 0.04, p = 0.22 (explosion: r << 0.01, p = 0.98)
Avg. wind speed	r = 0.34, p = 0.04	r = 0.12, p = 0.0001 (explosion: r = -0.005, p = 0.86)

In contrast to the WT1-specific results based on data from Site A, no statistically significant correlation is found between converter failure and ambient temperature in the case of Site D. While some correlation with the relative humidity is suggested by the monthly average data, the more reliable results obtained from the daily average data disprove this. A strong, statistically significant correlation is found between the number of failures and the average wind speed. A more detailed analysis based on the daily average wind speed shows that this applies only for the non-destructive failures. In contrast, explosion failure, which was earlier found to be strongly correlated with lightning strikes, is not correlated with the wind speed.

This is a very interesting result. It indicates that at least two different failure mechanisms are present in the converter of WT2: the first one leads to explosion failure and is strongly related to lightning strikes in the area of the wind park; the second one leads to non-destructive failure of the converter and is favoured by high wind speeds and therefore a high electrical loading of the wind turbine.

5.2 On-site operating conditions

5.2.1 Results for wind turbine WT1

Load profile

The 10-min-interval SCADA data available from the offshore Site A for the years 2009 and 2010 has been used to characterize the load profile of the turbines at this site.

Figure 34 (left) shows a typical histogram of the generated active power, normalized with the rated turbine capacity. According to this, the wind turbine

operates at or close to rated power (P ≥ $0.975 \cdot P_N$) at approx. 40% of the time. During approx. 25% of the time, the turbine does not generate power. Instead, it consumes some power (up to 1.4% of the rated power), e.g. for operating the control system and internal heating systems.
Figure 34 (right) shows a scatter plot of the produced reactive power over the active power generated by the turbine. The power factor of the power exported to the grid remains close to 1 over the whole operating range with P>0 of the turbine.

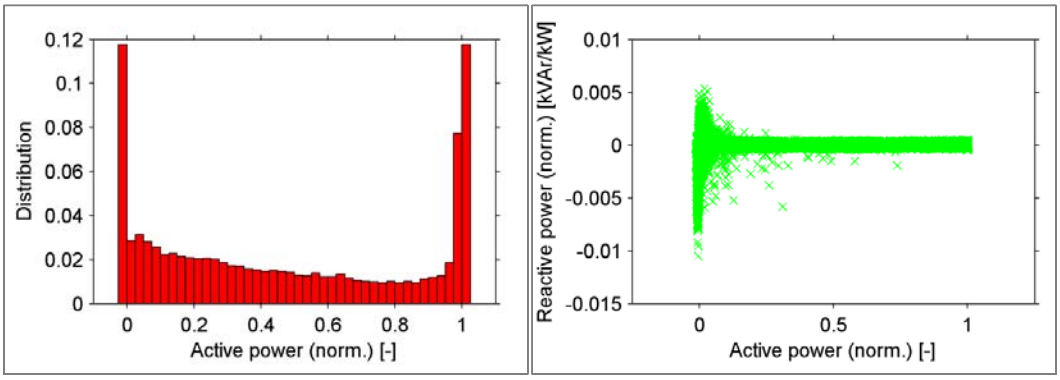

Fig. 34: Typical plots of the load profile (left) and reactive over active power (right) of a turbine located at Site A; both quantities are normalized with the rated turbine capacity

As discussed in detail in Section 2.4, a particularly reliability-critical operating condition for converters in DFIG turbines is the operation at high currents and low frequencies of the generator-side converter. However, the SCADA system of the WT1 turbine does not log the internal electrical operating conditions of the converter. Still, the frequency of the rotor current can easily be derived from the rotational-speed signal of the generator, using the fact that:

$$f_r = \frac{n_s - n_r}{n_s} \cdot f_e \tag{4}$$

Herein, f_r denotes the electrical frequency in the rotor, f_e is the electrical frequency of the applied stator voltage, n_s denotes the synchronous speed and n_r the rotational speed of the machine. With f_e = 50 Hz, n_s = 1500 rpm for a 4-pole machine and the rotational speed of the generator according to Fig. 35, the rotor frequency is found to vary between 0 and 8 Hz during normal turbine operation. Most of the time, the electrical rotor frequency is in the range of 7-8 Hz while frequencies around 0 Hz occur only during a small portion of the operational time of the turbine.

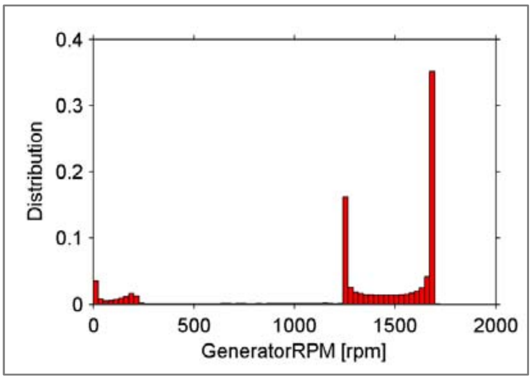

Fig. 35: Histogram of the rotational speed of a DFIG turbine at Site A

Temperature and relative humidity

In case of the WT1 system, some information regarding the thermal conditions inside the converter modules is found in the SCADA signals: These cover the 10-min average temperature values measured by the module-internal temperature sensor which is located next to the power devices on the DCB. Figure 36 shows typical plots of the grid-side (left) and the generator-side (right) module-internal temperature over the normalised active power. The temperature varies only in a very limited range of approx. 25…55°C and increases slightly with the active power generated by the turbines.

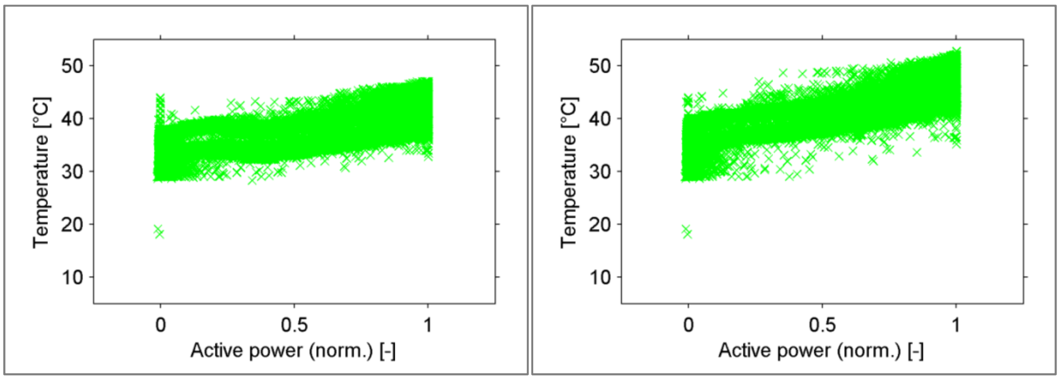

Fig. 36: Values of the module-internal temperature over the generated active power for a grid-side module (left) and a generator-side module (right) of a WT1 system at Site A

Figure 37 (left) shows the variation of the above introduced grid-side module temperature over a period of two years. As a comparison with the corresponding nacelle temperature in Fig. 37 reveals, the module temperature is maintained at temperatures between approx. 25°C and 40°C during the colder seasons and reaches slightly higher temperatures during the summer.

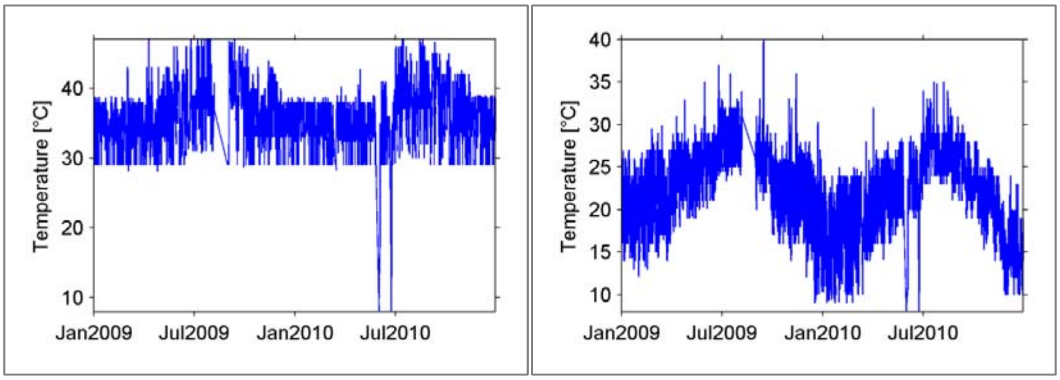

Fig. 37: Seasonal variation of the grid-side module temperature (left) and the nacelle temperature (right) in a WT1 turbine at Site A

As described in Section 4.2, the operating conditions inside the converter cabinets of single onshore and offshore turbines have been explored by means of temperature and humidity loggers.

Figure 38 shows the conditions measured at a WT1 turbine at the onshore Site B. Similar results have been obtained from a second WT1 system at the same site.

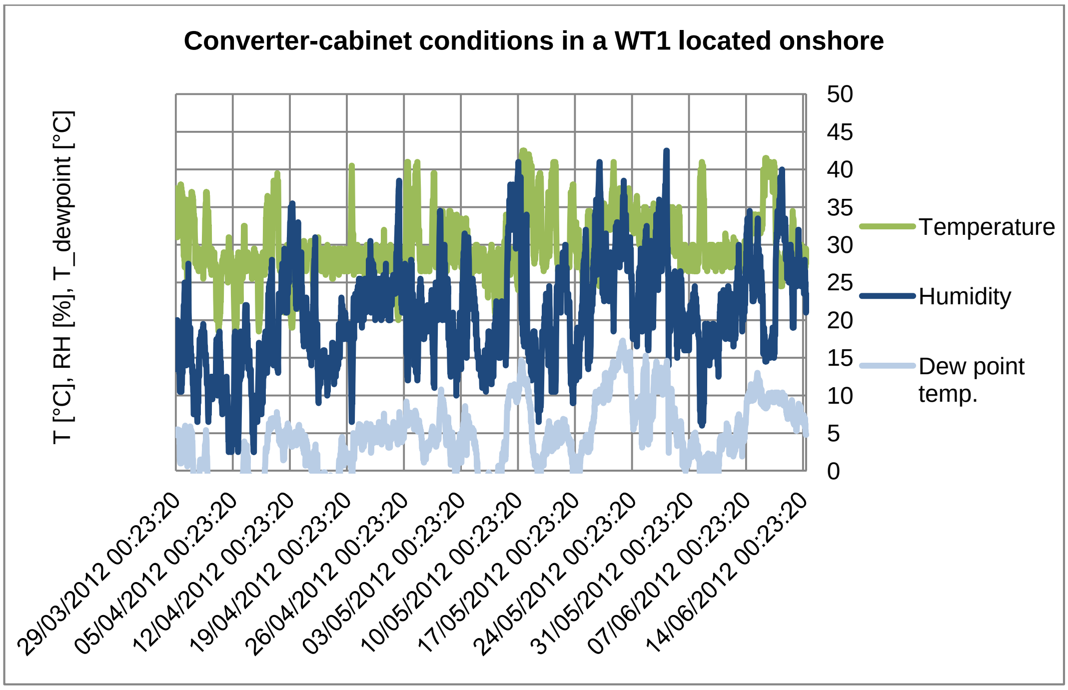

Fig. 38: Temperature, relative humidity and corresponding dew-point temperature inside the converter cabinet of a turbine of type WT1

The finding that the thermal operating environment of the converter modules is not critical in the WT1 system is confirmed by the maximum-temperature data collected by means of thermo-sensitive tape: Both on the top-cover of the converter modules and at the side of the heat sink, for the grid-side and the generator-side modules, maximum temperatures in the range of 43-60°C have been found. In a single case, a maximum value of 65°C was measured on the heat sink of a generator-side module. Again, this does not provide any signs of overheating of the modules during turbine operation. Initial speculations that the cooling of the converter cabinets might be insufficient can, at least for the period April to June monitored within the present project, therefore not be confirmed.

A particularly interesting case could be logged on a WT1 turbine at the offshore Site A, see Fig. 39: After a standstill period of 9 days and 2 days of major repair work with an opened nacelle (see the red-marked area in Fig. 39), a converter failure occurred during start-up of the turbine on 4 May. Similar cases were reported to have occurred before in the same offshore wind park. The logged temperature and relative-humidity data confirm that this most likely is related to condensation: Due to the standstill period, the nacelle cooled down and the relative humidity increased to values of approx. 60%. This results in a low difference between the temperature logged the top inside of the converter cabinet and the corresponding dew-point temperature, which is likely to have caused condensation on the converter modules having a high thermal inertia.

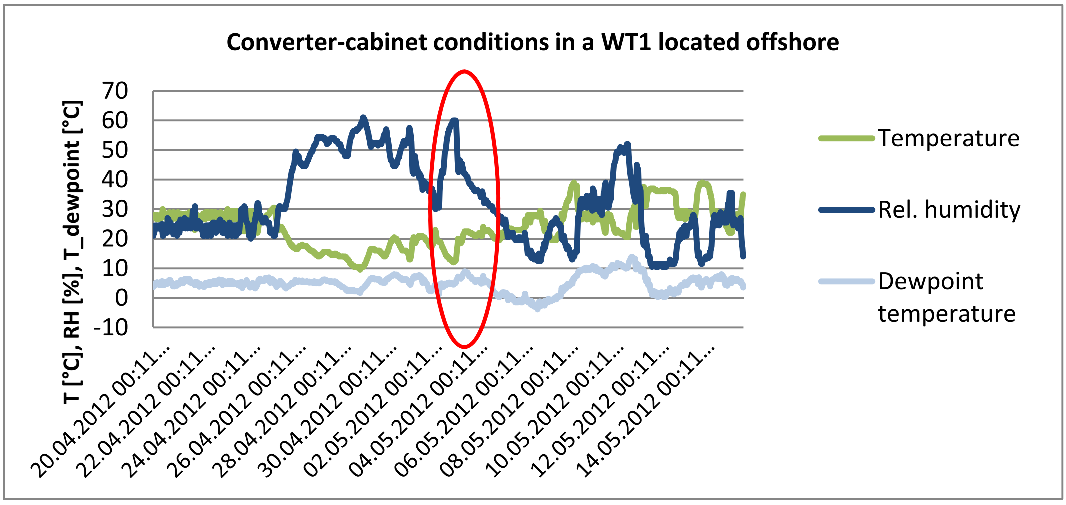

Fig. 39: Temperature, relative humidity and corresponding dew-point temperature inside the converter cabinet of a WT1 turbine with long standstill period

In summary, it can be stated that the converter operating conditions are uncritical during normal turbine operation but appear to be problematic with respect to condensation after long periods of standstill.

Vibration

An impression of the vibration environment in which the converter modules are operating is provided in Fig. 40. This shows the acceleration spectrum measured on the heat sink of a converter module on a WT1 turbine at Site A in different operating points. The frequency range is limited to the frequencies below 1 kHz, which are considered to be the relevant frequencies with respect to mechanical impact on the converter. Note that, according to information from the manufacturer of the vibration condition-monitoring system used for the measurements, the amplitudes in this spectrum can contain an error of up to 15%.

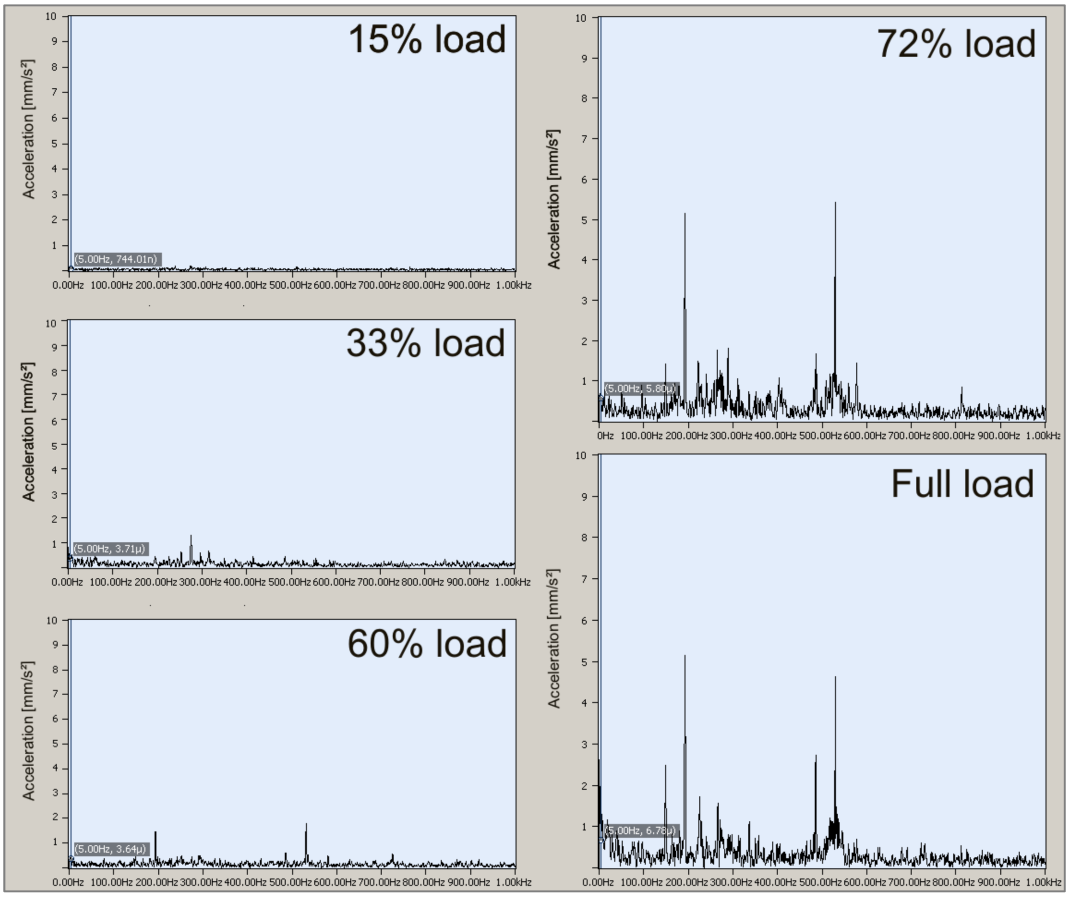

Fig. 40: Acceleration spectrum measured on a converter module of a WT1 at Site A at different loads

Not surprising, Fig. 40 shows a strong increase in the acceleration level from low to high load, while little difference is found between the 72% and the full-load point. In the upper load range, peak acceleration values are observed at frequencies close to 200 Hz and 530 Hz. However, the observed maximum levels of acceleration remain far below the levels applied during reliability-testing at the manufacturer.

5.2.2 Results for wind turbine WT2

Load profile

The 10-min-interval SCADA data available from the offshore Site D for the years 2009 and 2010 has been used to characterize the load profile of the turbines at this site.
A typical histogram of the generated active power is shown in Fig. 41. According to this, the wind turbine operates at or close to rated power ($P \geq 0.975 \cdot PN$) at approx. 23% of the time. During approx. 27% of the time, the turbine does not generate power. During periods of no production, the turbine consumes up to approx. 1% of the rated power.

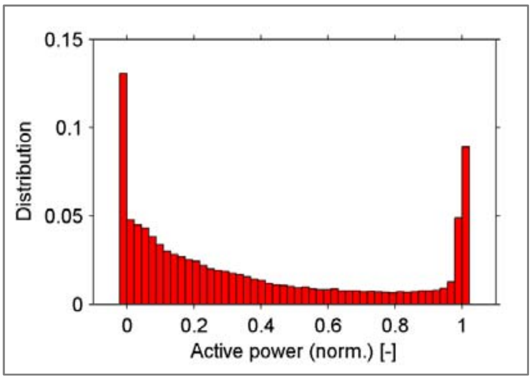

Fig. 41: Typical load profile of a turbine located at Site D, normalized with the rated turbine capacity

For the same turbine, Fig. 42 (left) shows a scatter plot of the produced reactive power over the active power generated by the turbine. Figure 42 (right) provides the same for an adjacent turbine in the same radial.

A comparison with the corresponding plot concerning the WT1 system in Fig. 34 makes clear that the amount of reactive power provided to or consumed from the electric power grid is considerably higher in case of WT2. However, the amount of reactive power requested from different turbines at Site D shows substantial differences, as a comparison of the plots in Fig. 42 demonstrates.

While Fig. 42 (left) represents the situation on the turbine with the highest number of converter failures in the wind park, Fig. 42 (right) is from a turbine without any converter failures in the investigated period. Based on the observed discrepancy and the fact that the loading of the converter-internal diodes increases with the reactive power, an interesting question is if there is a correlation between the number of converter failures on a turbine and the amount of reactive power requested from this turbine. To clarify this, a linear correlation analysis of the number of failures per turbine and the average amount of reactive power requested from the turbine was carried out for the whole park. However, no statistically significant correlation between these quantities was found.

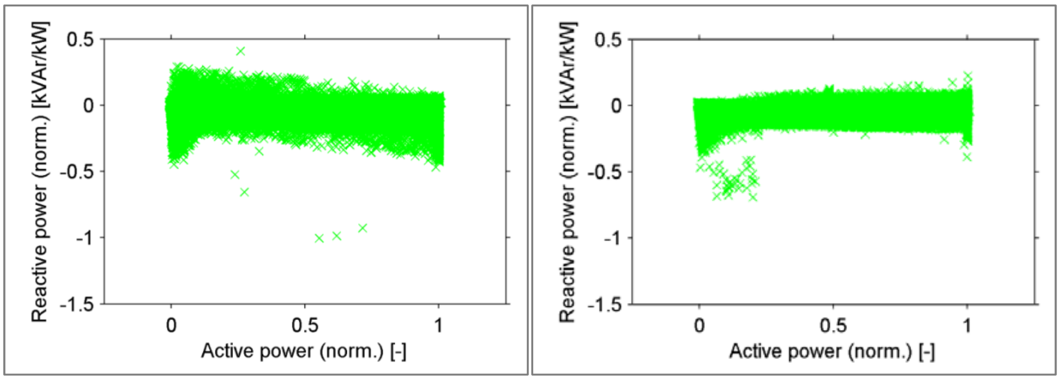

Fig. 42: Scatter plots of reactive vs. active power from a WT2 system with (left) and without (right) converter failures; quantities are normalised with the rated turbine capacity

Temperature and humidity

In case of the WT2 system, no information regarding the thermal conditions inside the converter modules was contained in the provided SCADA data. From single available screenshots containing converter-temperature data, at least a rough estimation of the thermal conditions was possible. According to these, the coolant temperature is typically in the range of 30…45°C, while the so-called "board temperature" of the converter ranges between approx. 20…50°C when the turbine is in operation. During standstill periods, the coolant temperature is actively maintained at 15…25°C and the board temperature remains within the same range as during operation.

Also in case of the WT2, the operating conditions inside the converter cabinets of single onshore and offshore turbines have been explored by means of temperature and humidity loggers. Figure 43 shows the conditions measured at a turbine at Site D.

The converter-cabinet temperature is found to range between 25 and 50°C, while the relative humidity remains below 40%. The dew-point temperature lies significantly below the measured temperature at all times so that there is clearly no risk of condensation during normal operation.

Thus, also in the case of the WT2, no exceptional conditions are found inside the converter cabinet which would be likely to favour converter failure.

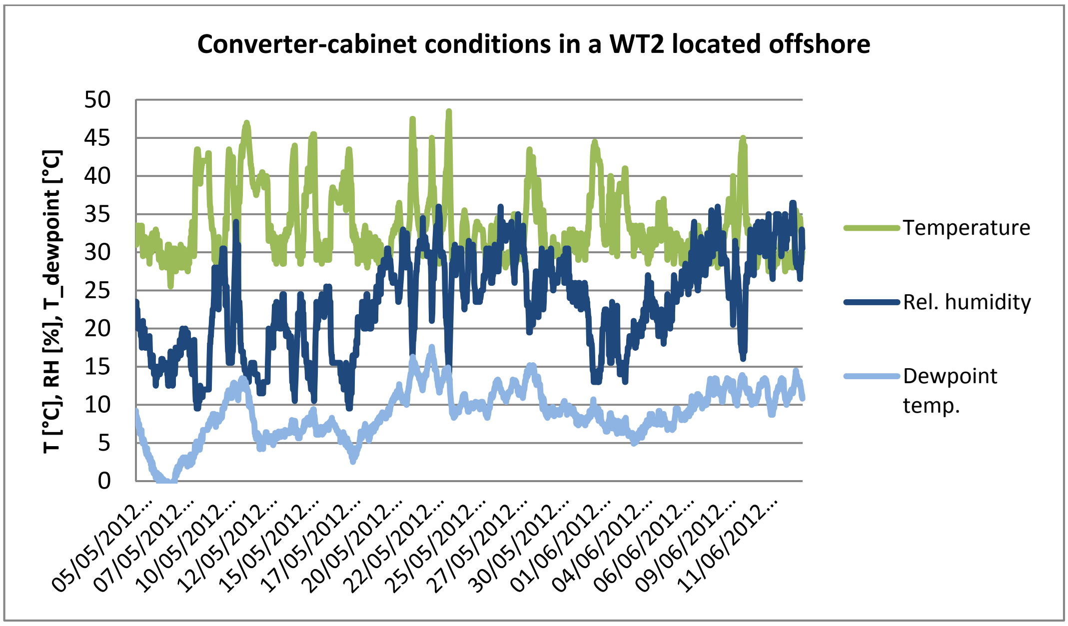

Fig. 43: Temperature, relative humidity and corresponding dew-point temperature inside the converter cabinet of a WT2 turbine at Site D

5.3 Post-operational investigation of converter modules

5.3.1 Electrical measurements

Nine converter modules from Site A without obvious signs of damage were investigated in several tests and measurements throughout the project, see also Section 4.3. Among the nine modules were four grid-side and five generator-side modules. While all grid-side modules had been tested before and were known to be defect, the condition of the generator-side modules was unknown. All of them had been replaced in relation with failure of the converter.

Table 7 summarises the results of the measurements described in Section 4.3.

The four grid-side modules were found to have the following defects:

- Non-switching top IGBTs (1 case)
- Non-switching bottom IGBTs (2 cases)
- Failed current and temperature sensors (1 case)

Among the generator-side module, a single failed one was found, with non-switching bottom IGBTs. All modules met the specified withstand voltage of 1200 V.

Table 7: Results of the electrical measurements

Measurement	Comment	Values / results
IGBTs	functionality test top IGBTs	1 not switching, 8 functional
	functionality test bottom IGBTs	3 not switching, 5 functional
Diodes	functionality test top diodes	all functional
	functionality test bottom diodes	all functional
Temperature sensor	functionality test	1 defect, 8 functional
Current sensor	functionality test	1 defect, 8 functional
Withstand voltage	measured at 2.35 mA	1275-1375 V
Voltage drop	over the IGBTs	50 A: 0.77-0.80 V 200A: 0.93-0.96 V
	over the diodes	50 A: 0.75-0.78 V 200A: 0.94-0.97 V
Insulation resistance	between cooling fins and DSUB	7.5 -10 MΩ
	between cooling fins and AC, DC+ and DC- terminals	approx. 5 – 100 kΩ
	between cooling fins and heat sink	100- 360 GΩ (900 GΩ for one very clean module)

Because of the fact that all tests and measurements were performed on complete modules, it was not possible to test single-chip functionality. Due to the same reason, it was not possible to distinguish if the non-switching of IGBTs were caused by a defect gate-driver board or by failed IGBT chips.

Diodes fail typically in short-circuit mode. In spite of the parallel connection of a large number of diodes inside the modules, it can therefore be concluded from the diode functionality-test that all of the diodes are intact.

The measurement of the voltage drop over the IGBTs and the diodes was carried out with currents of 50 A, 100 A and 200 A in case of the 4-fold generator side modules. To obtain comparable results, only 75% of these currents were used in case of the 3-fold grid-side modules. The voltage drop and the differential resistances of both the functional IGBTs (R_{CE}) and the diodes, which were determined from the measurements, were found to be in satisfactory agreement with the datasheet values.

Finally, the insulation resistances between the cooling fins of the gate-driver board and the AC terminals, the DC terminals, the outside of the DSUB connector and the heat sink were measured. An interesting finding was that there is a galvanic coupling between the cooling fins and either an AC or a DC terminal. The marginal conductance between the cooling fins and the heat sink can be ascribed to surface contamination of the modules.

5.3.2 Forensic analysis

Analysis of destructed modules

A comprehensive analysis of two grid-side converter modules with severe signs of energy release was carried out within the project, using visual and optical microscopy inspection, an optical inspection as well as a scanning electron microscope. The results are presented and discussed in the following.

In both modules, the centre of destruction was located in one of the outer half-bridges, the surrounding plastic case was destroyed by the detonation and large amounts of soot were found inside and on the surface of the module, see also Fig. 44.

Fig. 44: Destructed converter module

In the first investigated module, clear evidence was found of high-voltage flashover between one cooling fin soldered to the gate-driver board and a screw fixing one of the half-bridges to the heat sink, see Fig. 45.

The dielectric strength of air is approximately 3 kV/mm. Thus to initiate a flashover over a gap of 7mm between the cooling fin and the screw, a voltage of approx. 20kV and therefore a multiple of the normal operating voltage of <1kV is required. The material transferred from the cooling fin to the screw indicates that the cooling fin must have been on a high negative potential with respect to the screw (which is assumed to be on ground potential due to its connection to the heat sink).

Four possible scenarios that might have caused the observed damage were discussed:

(1) A lightning strike hitting the surrounding structure found a discharge path through the converter module. The galvanic coupling between the power circuit and the cooling fin revealed by the electric measurements described in the previous section supports this possibility.

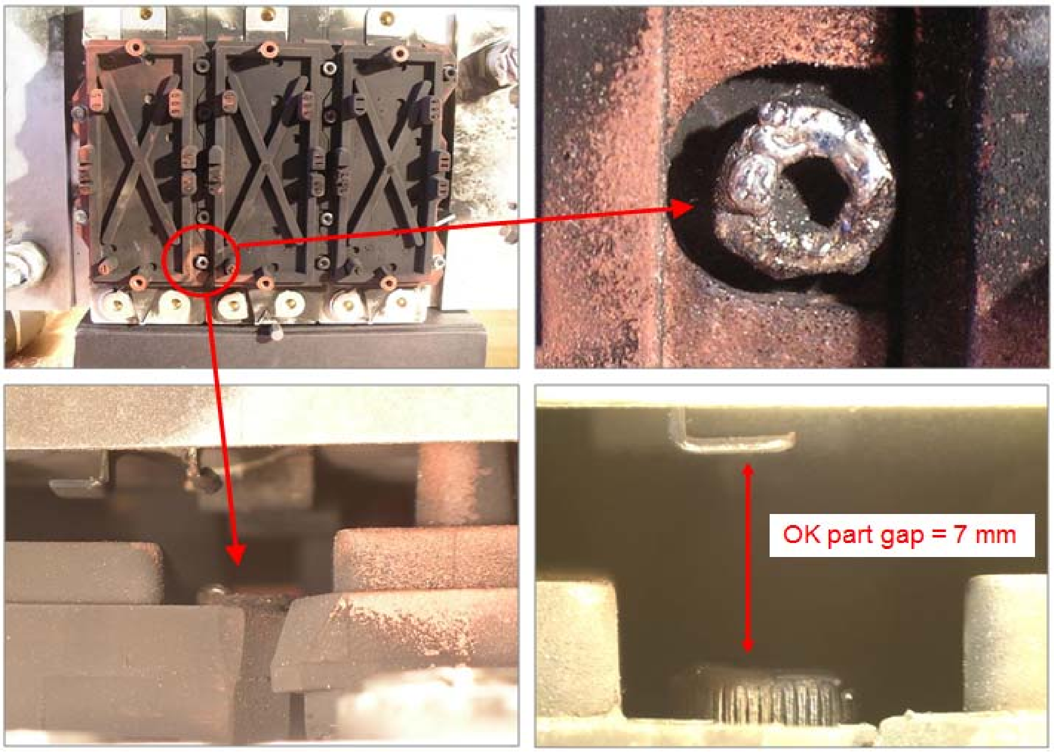

Fig. 45: Evidence of high-voltage sparkover between a PCB cooling fin and a screw reaching into the heat sink

(2) A disturbance in the external transmission grid occurred and the system failed to ride through the fault.

(3) Static electricity build-up from the rotor blades of the turbine found a discharge path through the module. The energy involved in that case would be too low to cause the level of damage observed, but it might initiate an arc-flash event. This phenomenon is known from airplane propellers and helicopters especially if rotor blades are of composite material. Once an arc-flash event is initiated, a lower voltage level is sufficient to maintain it. A considerable amount of energy with the potential to cause the severe damage observed is typically available in the DC link of the wind-turbine converter. However, static electricity build-up from the rotor blades is an unlikely cause of high voltages in the converter as an electricity build-up is usually drained through slip rings on the turbine shaft.

(4) A reduction of the air gap by a foreign object could have initiated an arc flash, which subsequently might have been maintained in the way discussed above. A likely foreign object is e.g. an insect creeping into the open module. Bartram [26] showed that flies are attracted by the silicone gel typically covering the power devices in wind-turbine converters. In spite of the often large distances from the coast, high amounts of insects

have been found inside the turbines and even inside the converter cabinets at another offshore wind park (Site D, see Fig. 46).

Fig. 46: Dead insects found inside wind turbines at offshore site D, confirming the presence of insects also at larger distances from the coast

In the context of the described flashover damage, the air gap between the cooling fin and the screw is considered relatively small. Besides using a design with larger air gap, a measure to prevent flashover in this part of the module could be the introduction of a thin insulating sheet of e.g. Kapton or Mica in the gap.

A second finding from the forensic analysis of the first module was that high currents must have been present also in the signal contact springs connecting the PCB with the power devices. This could be concluded from discolorations and small damages in the contact area.

Not surprisingly, also the analysis of the second destructed module revealed signs of very high currents through the module. As visible in Fig. 47, all three paralleled half-bridges show the same damage pattern: The connections to the DC+ and the AC side show melting in the same contact points. The considerable displacement of the DC- connection from the DC+ connection observed in Fig. 47 gives evidence of a very strong energy release.

Another potential failure mechanism resulting in destruction, which was discussed in the root-cause analysis in this project, is a resonance of the spring contacts. This might lead to intermittent loss of the contact between the gate-driver board and the IGBTs and therewith cause a so-called "floating gate" in the IGBT, i.e. a state between ON and OFF. A floating gate in an IGBT results in a strong heat-up and leads finally to thermal destruction.

A second way in which vibration can lead to loss of contact is the mechanism of fretting corrosion, as discussed in Section 2.2. During the forensic analysis of the first module, some indication of fretting was found on the gold contacts of the PCB. It is, however, considered possible that the observed damage is instead a result of the strong mechanical forces acting during the energy release. A microscope inspection of the PCB gold contacts in the second module did not reveal any signs of fretting corrosion.

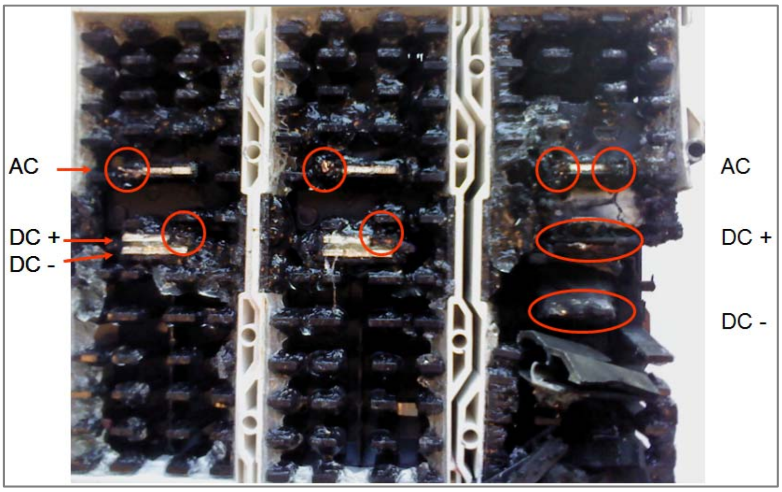

Fig. 47: Identical melting-damage pattern at the connections to AC and DC+ in all three half-bridges

In one of the destructed and in several non-destructed modules, a deterioration of the thermal grease was observed. The grease appeared to be relatively dry and seemed to have been applied in relatively small amounts, not completely covering the interface area of DCB and heat sink (see Fig. 48). A deterioration of the thermal grease can cause an increase in the thermal resistance to the heat sink and in this way lead to over-heating of the power devices.

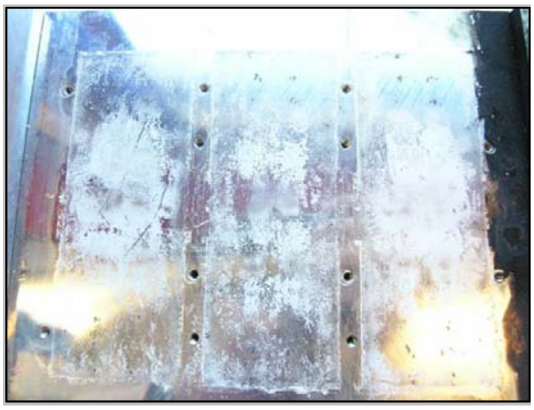

Fig. 48: Degraded thermal grease between DCB and heat sink

An initially surprising finding was the discovery of dark, corroded spots at the bottom side of the DCB (see Fig. 49a and b) as well as on the upper side of the non-anodized aluminium heat sink (Fig. 49c). In the area of these spots, no thermal grease is left between the two surfaces. The chemically inert gold-layer covering the bottom side of the DCB is damaged.

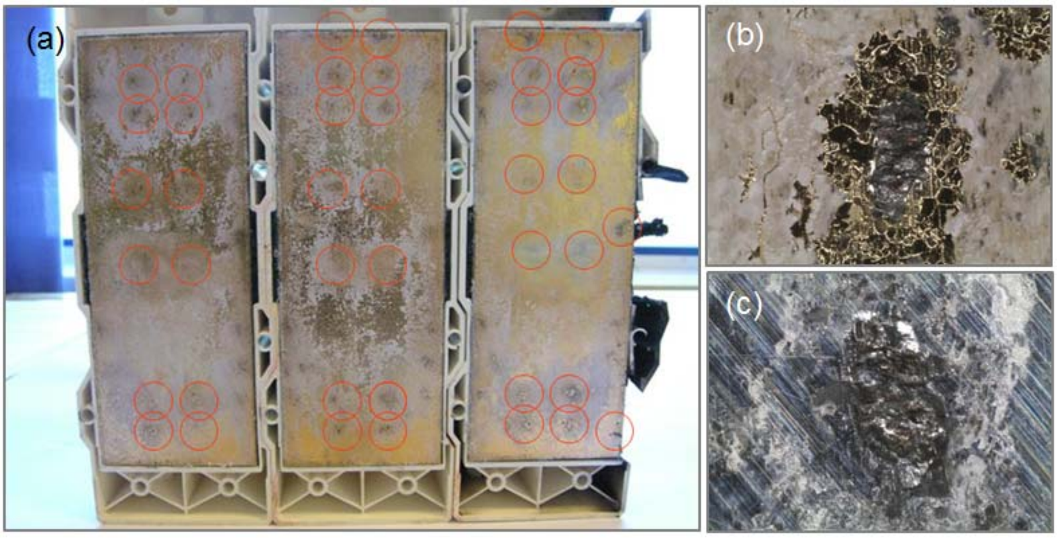

Fig. 49: Spots on the bottom side of the DCB and on top of the heat sink

In-depth analysis of one of the spots on the DCB was carried our using a scanning electron microscope. The analysis results, presented in Fig. 50, show that the spot predominantly consists of aluminium and copper, i.e. of material from the heat sink and the DCB. No traces of chlorine were found, which could have pointed to the ingress of salt.

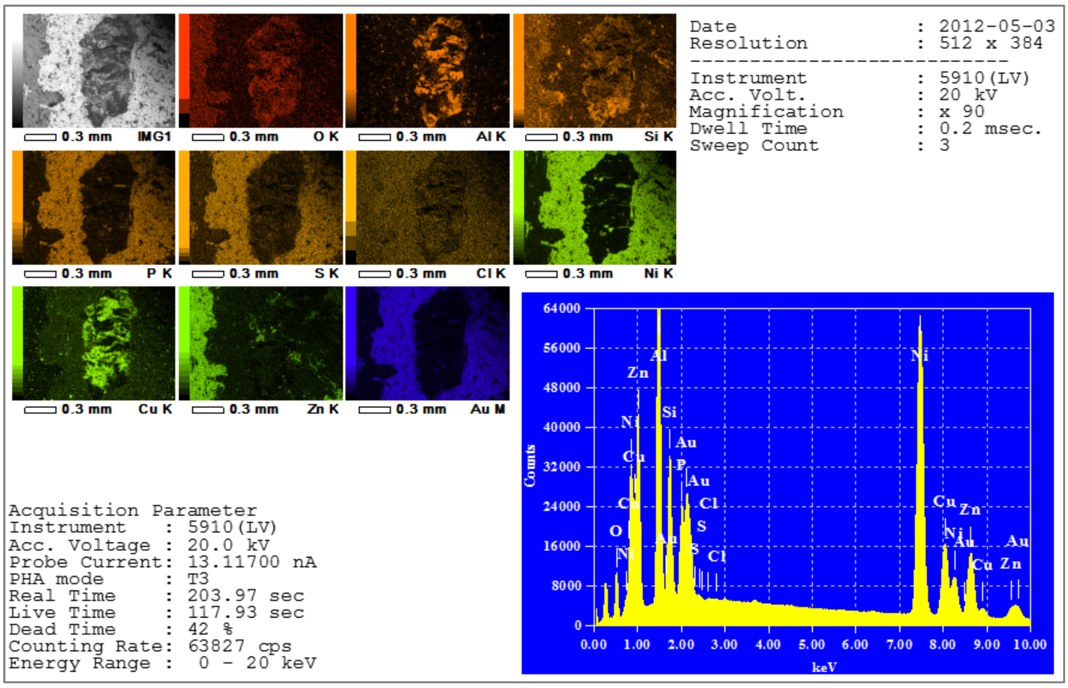

Fig. 50: Scanning-electron microscopy analysis of spots on the bottom-side of the DCB

The positions of the dark spots coincide with the points in which the DCB is pressed to the heat sink by means of the plastic pins visible in Fig. 47. In combination with the chemical composition of the spot, this observation strongly suggests the presence of fretting corrosion: Under the impact of mechanical pressure, thermal cycling and possibly also promoted by vibration, abrasive wear of the two surfaces takes place.
The craters caused by this effect were found to reach no further than approx. 75µm over and into the DCB surface. This is not considered critical for the integrity of the DCB.

Unless the observed fretting process causes an increased thermal resistance, it is not considered a reliability-critical phenomenon. It is recommendable to clarify this in the future. A possible countermeasure concerning the formation of the observed spots could be the anodising of the aluminium surface. Anodising is an electrolytic passivation process converting the aluminium surface to aluminium oxide, which has an increased corrosion and wear resistance. Also a finer structure of the heat-sink surface might reduce the formation of fretting spots.

In case of the second destructed module investigated, the undamaged remaining two half-bridges were investigated in detail using an optical microscope. The pictures displayed in Fig. 51 were taken through the silicone gel covering the power devices in order to discover possible signs of bond-wire corrosion, bond-wire lift-off or chip-solder damage.

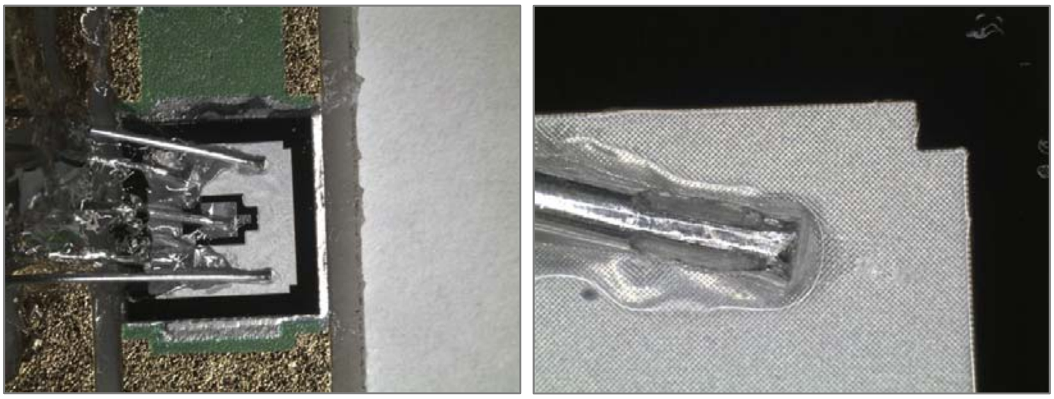

Fig. 51: Microscopy inspection of the bond-wires and die attach

Besides the classical thermo-mechanical mechanisms leading to bond-wire fatigue or lift-off, also vibration can have this effect: Previously in another application area, the formation of standing waves in the silicone gel lead to bond-wire fatigue. In that case, the problem could be solved by integrating a plastic grid into the gel which suppressed the formation of standing waves.

Bond-wire corrosion can occur due to the highly permeable properties of the silicone gel covering the chips, as is known from other areas of application. Gaseous sulphur, which can e.g. evaporate from rubber hoses or rubber seals, can permeate through the gel layer and lead to severe corrosion of the bond wires. In the converter modules used in the WT1 turbine and investigated here, the silicone gel is not protected by the module housing, instead it is in free contact with the surrounding air. However, the microscope analysis which provided Fig. 51 did not reveal any irregularities of the bond-wires or the die-attach.

As described in Section 2.2, also a contamination of the PCB can be a cause of converter failure. The investigated converter modules were therefore thoroughly checked for signs of contamination or corrosion. Neither salt nor dirt nor corrosion was visible on the bottom-side of the PCB in these cases. A contamination which was discussed in the root-cause analysis and which is possibly not visible for the bare eye might be caused by glycol spill from coolant spill onto the modules: After the water has evaporated, the glycol remains on the PCB and can lead to a deterioration of the insulation capability of components on the PCB.

While the bottom-side of the PCBs in the investigated modules could be inspected, the PCBs were found to be completely moulded by a hard coating on the upper side. This is an effective measure to prevent any contamination, corrosion or other potential reduction of the creepage distance on the upper side of the PCB. However on the other hand, hard moulding-compounds are known to introduce thermo-mechanical stress and to hinder the dissipation of heat from the PCB. This is a potential reliability-critical aspect which might be of interest for future analysis.

Finally, the formation of tin whiskers in systems containing lead-free tin was introduced in Section 2.2 as a potential cause of converter failure. The modules used in the WT1 system are known to contain only lead-free tin. In spite of that, tin whiskers were not found in any of the analysed modules. Due to the abovementioned moulding of the PCB on the upper side and the use of gold pads for providing the electrical connection to the spring contacts on the bottom side of the PCB, the formation of tin whiskers is considered unlikely in the investigated type of modules.

Analysis of non-destructed modules

In addition to the analysis of two severely damaged modules described above, two grid-side converter modules without any visible signs of destruction were investigated at Swerea IVF, Göteborg.
In the following, the key results of this analysis are presented. Major parts of the text as well as all pictures in this subsection are taken from the analysis report [36] and reproduced here by courtesy of Swerea IVF.

The investigation comprised the following analysis techniques:

- X-ray microscopy inspection of driver board (PCB) and IGBT/diode half-bridges
- Visual/optical inspection (stereo microscope) of the observable side of the partly encapsulated driver board, and of the IGBT/diode bond-wire appearance in uncovered half-bridges

- Scanning acoustic microscopy (SAM) inspection of the IGBT and diode chips in the half-bridges with respect to possible die attach solder cracking
- Optical microscopy inspection of cross-sectioned IGBT chips with respect to the die attach integrity
- Scanning electron microscopy / energy dispersive spectroscopy (SEM/EDS) analysis of corrosion/contamination

The primary objective with the present failure analysis was to investigate if the converter-module malfunctions could be connected to fatigue-related damages in the half-bridges, specifically to crack formation in the die-attach solder of the IGBT and diode chips, or to bond-wire fractures. In addition, a general inspection of the driver board was included.

Removal of the silicone potting compound covering the half-bridges could not be fully carried out due to difficulties in finding an appropriate silicone stripper formulation. However, a careful mechanical removal of the silicone compound down to the vicinity of the bond wires facilitated the investigation.

Table 8: Analysis steps performed on the two investigated modules

Object	Converter-module type	Analysis steps
#1	3-fold grid-side module, manufactured in 2006	• Visual inspection of driver board (one side) • X-ray inspection of driver board • X-ray inspection of half-bridges • SAM inspection of chip die-attach solder in half-bridges • SEM/EDS analysis of observed corrosion / contamination • Full manual/mechanical check of bond wire integrity in half-bridges
#2	3-fold grid-side module, manufactured in 2006	• Visual inspection of driver board (one side) • X-ray inspection of driver board • SAM inspection of chip die-attach solder in half-bridges • Partial manual/mechanical check of bond wire integrity in half-bridges • Cross-section of IGBT chips for check of die attach solder (verifying SAM results)

Converter module #1

Figure 52 shows an overview optical image of the driver board in converter module #1. At the marked location, contamination and likely corrosion products could be observed. Figure 53 shows detailed images of the affected parts of the driver board and an adjacent spring connector:

Contamination/corrosion products were observed on the driver board between a component pad and a connector pad (Fig. 53a and b), indicating a possible path of electrical conduction during field operation. Figure 53c shows contamination/corrosion products on the corresponding pin connector to the half-bridge (marked with an arrow). Further contamination spots were observed at several positions on the driver board (Fig. 53d-f).

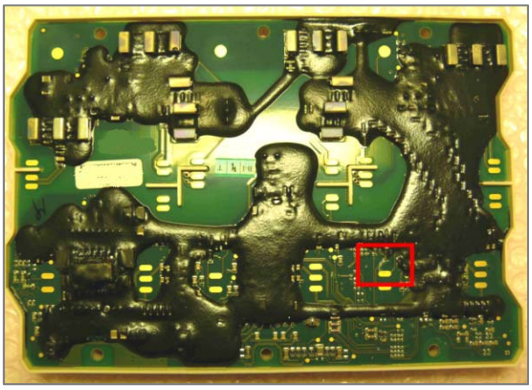

Fig. 52: Driver board of converter-module #1 after dismantling (bottom side) with marked location of observed contamination and likely corrosion products

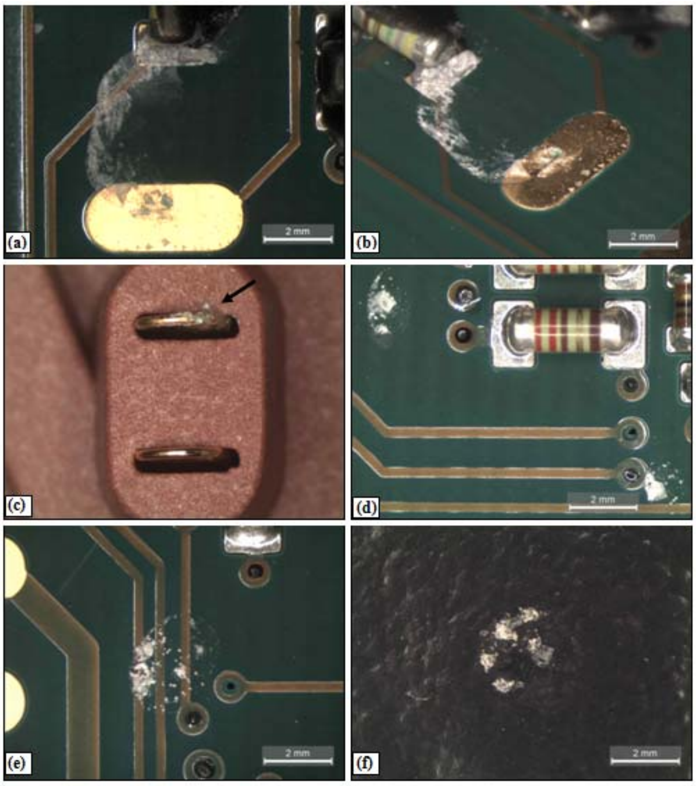

Fig. 53: Optical inspection images of converter module #1, (a, b) contamination/corrosion products on driver board between component pad and connector pad, (c) corresponding pin connector, (d-f) contamination spots observed at several positions on the driver board

A SEM/EDS analysis of the contamination revealed the presence of sodium (Na) and chloride (Cl), indicating impact from the sea based environment, i.e. moisture and salt. The SEM/EDS analysis of the contamination/corrosion products observed between component pad and connector pad (see Fig. 54) showed a dominant content of tin (Sn) and chloride (Cl) in addition to oxygen (O) indicating corrosion products. These form a possible path for electrical (ionic) conduction during field operation.

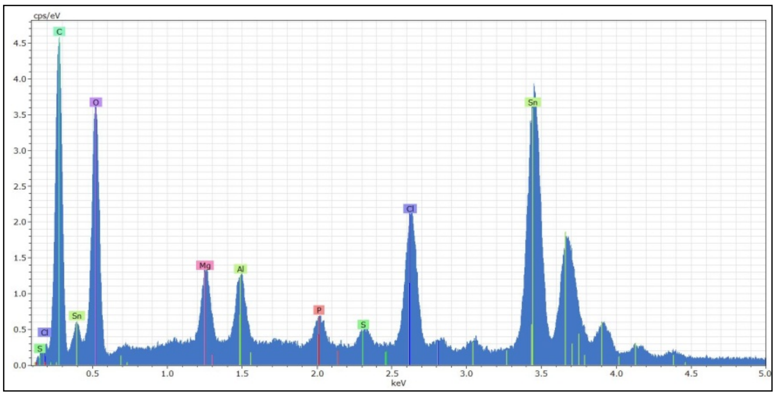

Fig. 54: SEM/EDS analysis of contamination / corrosion products

Figure 55 shows X-ray images of various driver-board solder joints in converter module #1. These indicate a generally acceptable solder-joint appearance, apart from some solder spatter and some voiding in solder joints of passive components. However, X-ray inspection of the driver board via holes (Fig. 56) showed a somewhat uneven hole plating, in addition to a quite thin plating. Possibly this could be a reliability concern during temperature cycling / power cycling in field operation.

Figure 57 shows optical images of uncovered half-bridges in converter module #1. The chips and bond wires are visible under a remaining layer of silicone. The bond-wire integrity of every bond wire on all three substrates was manually / mechanically tested by careful pulling with a thin needle tool. This test showed that all bond wires in the half-bridges of converter module #1 were bonded satisfactorily to chips and substrate, respectively. A simultaneous visual inspection of the substrate plating could not reveal any plating damages or discrepancies, apart from a general slight colour shift of the gold plating on one of the substrates (the right substrate in Fig. 57a).

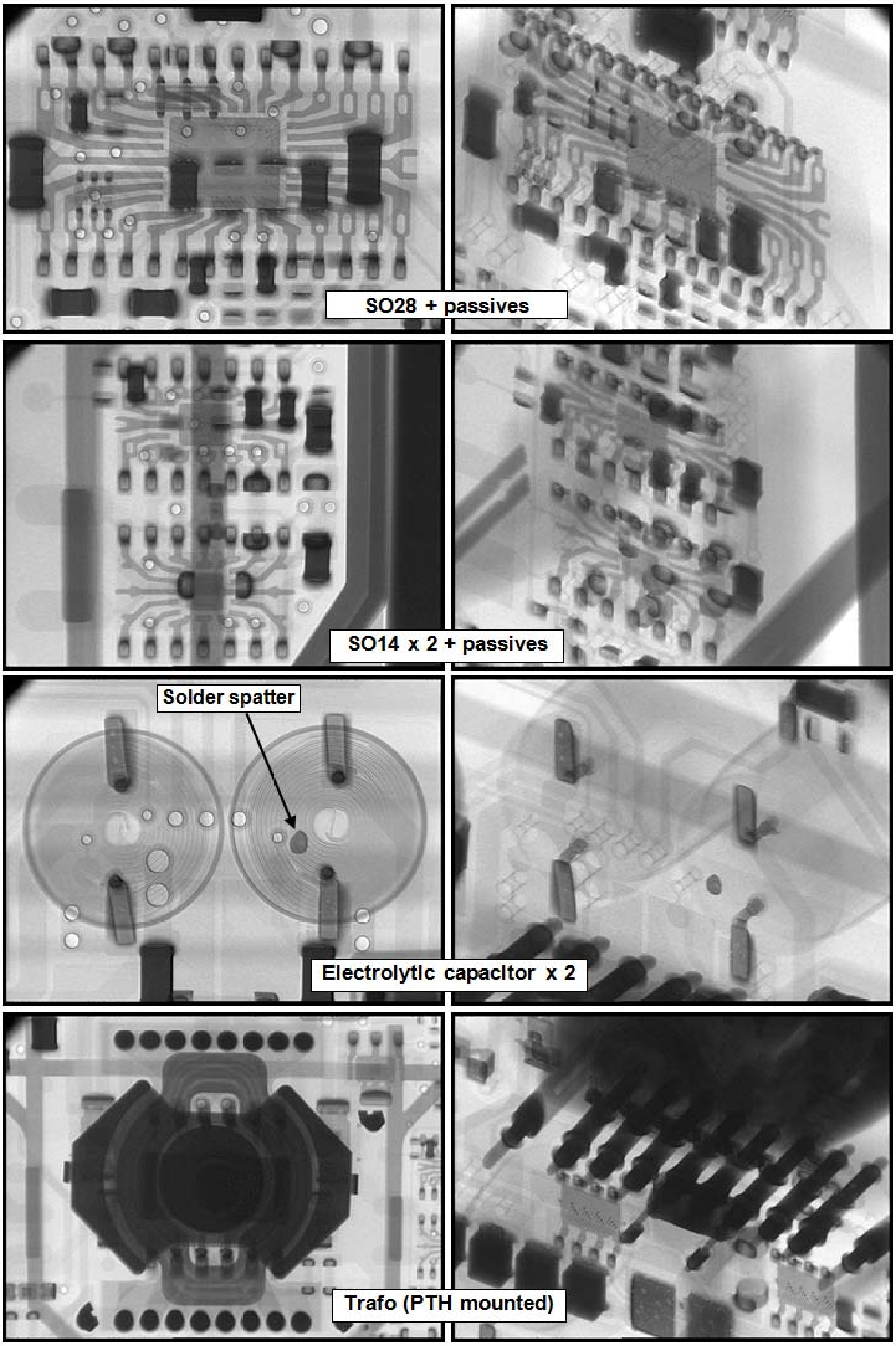

Fig. 55: X-ray images, top and oblique views, of driver-board solder joints in converter module #1

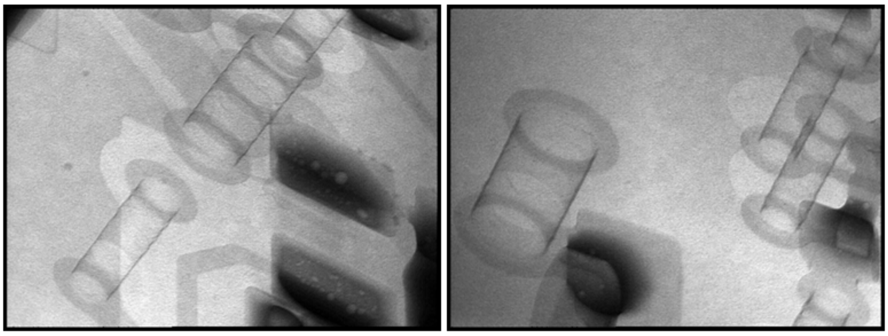

Fig. 56: X-ray images, top and oblique views, of driver-board via-holes in converter module #1

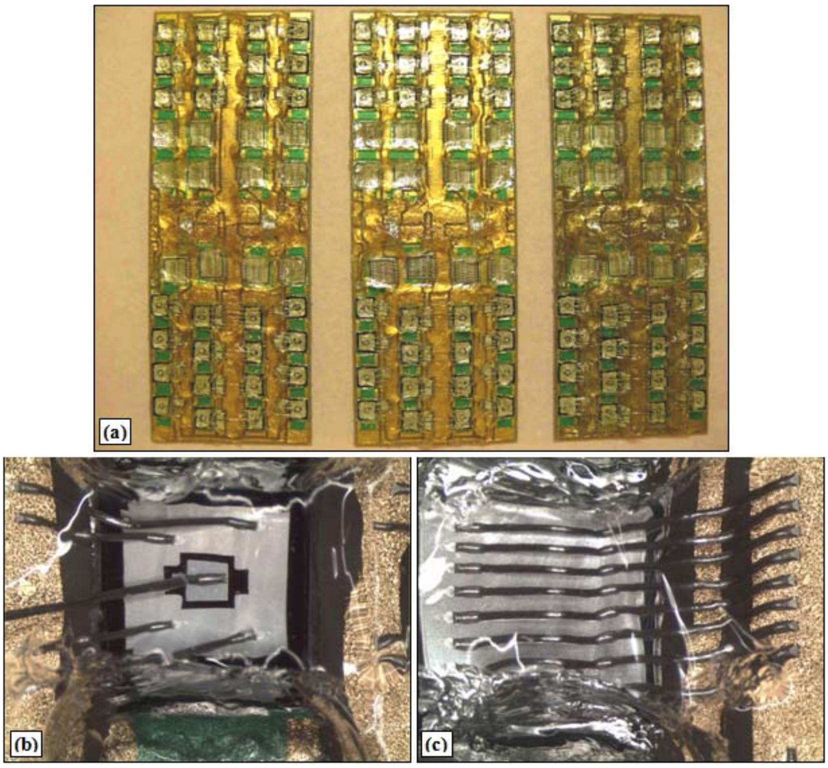

Fig. 57: Optical images of uncovered half-bridges in converter module #1, (a) overview of the three half-bridges with chips visible under a silicone layer (partly removed), (b, c) detailed images of chips and bond wires

Figure 58 shows an image from SAM analysis of the die-attach solder of the IGBT and diode chips of a half-bridge in converter module #1. All three half-bridges were investigated. The SAM analysis showed similar acoustic signal response from all chips in the three half-bridges, indicating intact die attach solder in all chips. The analysis was carried out from the backside of the half-bridges, i.e. through the substrate.

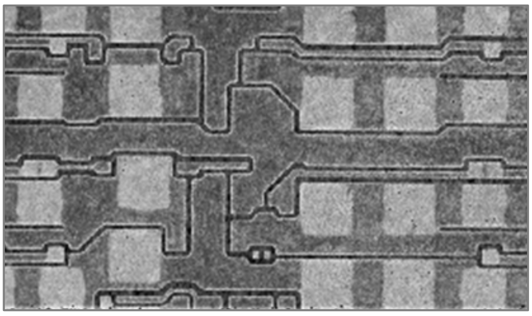

Fig. 58: SAM image (excerpt) showing a graphical representation of the acoustic signal response from the die-attach solder of a half-bridge

Converter module #2

Figure 59 shows an overview optical image of the driver board in converter module #2. In the marked area, re-melted solder joints were found during the optical inspection. Higher magnification inspection (Fig. 60) revealed severe re-melting in addition to a burned MELF (Metal Electrode Leadless Face) resistor.

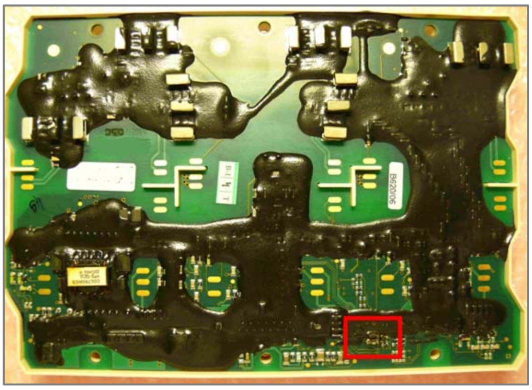

Fig. 59: Driver board of converter-module #2 after dismantling, with marked location of re-melted solder joints and "burned" components

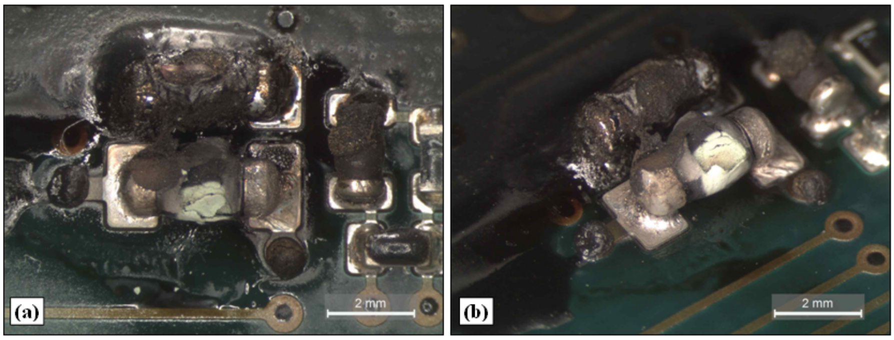

Fig. 60: Optical inspection images of converter module #2, top and oblique view of two resistors showing re-melted solder joints and damaged component package

An X-ray inspection (Fig. 61) of this area showed that also on the upper, moulded side of the driver board, joints were re-melted. Additional X-ray inspection of the driver board did not reveal any further damages or discrepancies of PCB components or solder joints. Apart from a somewhat uneven via-hole plating, the X-ray inspection indicated a generally acceptable solder joint appearance, similar to the solder joint appearance of converter module #1.

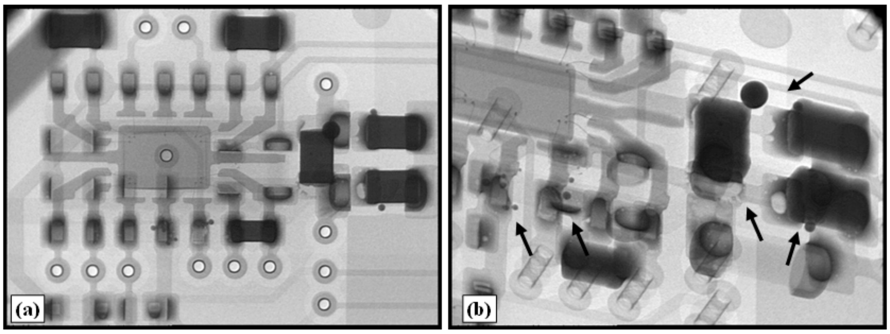

Fig. 61: X-ray image of driver board in converter module #2, top and oblique views revealing re-melted and broken solder joints at the resistors shown in Fig. 60, in addition to re-melted solder joints on the over-moulded side of the board

In the same way as in case of module #1, SAM analysis of the die-attach solder of the IGBT and diode chips in the three half-bridges of converter module #2 was carried out. This showed similar acoustic signal response from all the chips in the three modules, indicating intact die attach solder in all chips also in case of module #2.

In addition, a limited check of the bond-wire integrity, covering a selected number of chips and bond wires in the half-bridges of module #2. Also in this case, the manual / mechanical pull test showed that all tested bond wires were bonded satisfactorily to chips and substrate, respectively. In addition, the simultaneous visual inspection of the substrate plating did not reveal any plating damages or discrepancies.

Finally, Fig. 62 shows optical microscopy cross-section images of an IGBT chip from a half-bridge in converter module #2. The limited die-attach cross-section inspection of two IGBT chips revealed intact die-attach solder without any signs of crack initiation. The bond-wire connections showed largely satisfactory attachment, apart from small crevices at the bond-wire heel. This could be the initial stage of a fatigue crack, but could also have been caused by a not fully melted bond zone during the wire-bonding operation.

However in total, the cross-section inspection supports the observations from the manual / mechanical pull test of the bond wires and the SAM analysis of the chips' die-attach solder, according to which the observed module failure was neither caused by poor solder-joint quality nor by bond-wire damage.

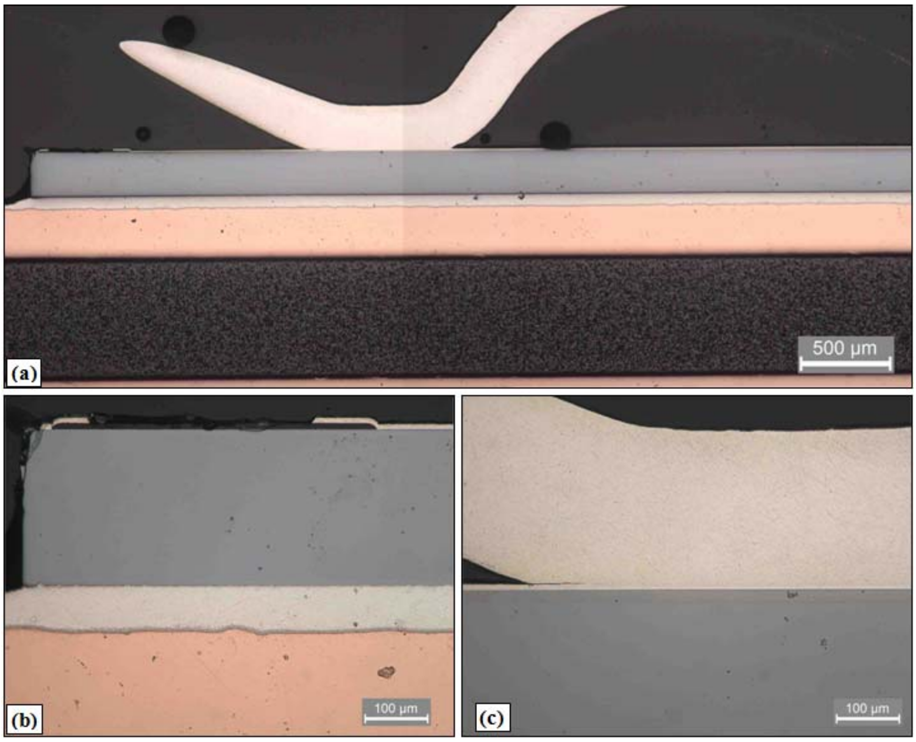

Fig. 62: Optical-microscopy cross-section images of a chip from converter module #2, (a) overview of part of the IGBT chip with wedge-bonded aluminium bond wire to the chip, (b) detailed view showing intact die attach solder, (c) magnified view of bond-wire connection to the chip metallization

The forensic analysis described in this subsection has shown that the failures of the two investigated non-destructed converter modules were neither caused by fatigue-related failures of the chip die-attach solder nor of the wire bonding. Instead, the investigation revealed damages/defects on the driver board in both analysed converter modules, possibly being the cause of the malfunction of these converter modules. However, in the case with re-melted solder joints and component damage (converter module #2), the failure might have had an external failure cause, such as lightning induced surge currents.

6 Result summary, conclusions and recommendations for future work

The objective of the study described here was to enhance the understanding of the failure modes and the causes of converter failures in two wind-turbine models, WT1 and WT2. In order to provide a basis for the identification of suitable countermeasures and of potential further investigation needs, the project has combined a variety of different approaches. These ranged from a literature study over failure-data analysis and an assessment of the on-site converter operating-conditions to post-operational investigation of converter modules.

Wind-power specific literature dealing with reliability issues of converters has been found to be sparse. Few publications are available on this topic to date. Among these, the main focus is on thermal-cycling issues in converters of DFIG wind turbines, in which the generator-side converter is subjected to high currents at very low frequencies and therefore to severe thermal cycling. However, the fact that Vattenfall has observed frequent converter failure not only in DFIG turbines but also in turbines with full-power converters suggests that the thermal-cycling issue might not be the key problem and stresses the importance of the data- and hardware-analysis based approach used in the present project.
A comparison of the available data for both wind turbine models WT1 and WT2, including onshore and offshore installations, has not confirmed the previously perceived higher failure rates of converters at offshore sites.

The key findings and conclusions from the analyses concerning the WT1 system are the following:

- The data analysis for Site A revealed a statistically significant correlation of the monthly number of converter failures with the monthly average ambient temperature. No significant correlation was found with the ambient relative humidity or with the monthly average wind speed.
- The investigation of the operating environment inside the converter cabinets did not reveal any signs of critical temperature or humidity levels during operation. However, it should be noted that the data-logging period was limited by the project duration to the months of April to June 2012, and that a continued monitoring over a whole year is recommendable.
- The electrical measurements performed on replaced modules have indicated different failure modes, each of which can be expected to have a variety of root-causes. The objective for future work should be to identify and remedy the most dominant of these. Concerning the failure-affected components in the converter modules, the electrical measurements suggest that the diodes are not susceptible to failure. A single case of sensor failure was found while the dominant failure-mode was the non-switching of IGBTs, which can be caused by both a defect in the gate-

driver board, the IGBT chips or the connections between these. The experience that IGBTs typically fail in a short-circuit mode, resulting in abrupt thermal destruction, suggests that in non-destructed modules the defect is located in the PCB or the connections and not in the IGBT chips. For future work, it is recommended to try to separately assess PCB, connection and IGBT failure. A potential collaboration with the module manufacturers is considered valuable for this and might significantly facilitate e.g. to separately test the functionality of the different module-components.

- The forensic analysis of the destructed modules revealed damage indicating the presence of voltages in the range of 20 kV, i.e. considerably above the converter operating-voltage. Lightning strike is considered a possible scenario. Due to the lack of lightning data for the region of Site A, no analysis of the correlation between failure and lightning was possible. On the background of the strong correlation of failure and lightning strikes obtained for Site D, it can be suspected that lightning also plays a relevant role for converter failure at Site A. The correlation of failure with higher ambient temperature observed at Site A might in fact be caused by a correlation with lightning strikes. In case lightning data can be acquired in the future, an analysis of the correlation with this factor is recommended.
- The degraded thermal grease and the large number of abrasion-wear spots in the heat-conducting area point to a possibly hindered heat dissipation from the power devices, which might cause overheating and / or accelerated ageing.
- The forensic analysis of the two non-destructed modules did not reveal any signs of fractures in the die-attach solder of the IGBT and diode chips, nor bond-wire fracture or substrate plating damages. This supports the impression that the classical fatigue-related reliability issues of power electronics play only a minor role for the frequent converter failures in wind turbines.
- In case of a single investigated module, contamination with salt and resulting corrosion was found on the PCB, which might have created a conducting path in field operation and is therefore a likely root-cause of the module failure. In the other investigated converter modules from Site A, no signs of corrosion or contamination with salt, coal particles or other dirt were found. As the single case of contamination with salt is not necessarily related to field operation but can also have been introduced during handling of the module, there is presently no clear evidence for an insufficient protection of the converter against the environment. However, this and in particular the theory that insects might creep into the converter modules and cause a sparkover should be further investigated. If e.g. insects can be found inside converter cabinets of WT1 (as it was the case for turbines of type WT2 at Site D), an enhancement of the protection would be an obvious and important countermeasure.
- Two further aspects worth investigating in the future are potential issues due to the hard moulding on top of the PCB and the question if in fact condensation-related failure takes place in spite of the current nacelle pre-heating routines.

In the following, the central findings and conclusions regarding the WT2 are compiled. For this turbine model, the investigations were based on, compared to the case of Site A, longer and more detailed sets of data from Site D as well as on the measured temperature and humidity conditions inside of single converter cabinets.

- The data analysis revealed a strong correlation between the daily number of lightning strikes in the Site D area and converter failure, particularly for the case of explosion failure. Another significant correlation was found between the daily number of (particularly non-destructive) failures and the daily average wind speed, i.e. the electrical loading of the converter.
- No correlation between the number of converter failures experienced by a turbine and the average reactive power provided by this turbine could be found.
- The investigation of the operating environment inside the converter cabinets did not reveal any signs of critical temperature or humidity levels. Also in the case of the WT2, the data-logging period was limited to the months of April to June 2012 and continued monitoring over a whole year is recommendable.
- The above summarised observations suggest sudden death by electrical overstress to be a relevant cause of failure in the WT2 system at Site D. However, it is a known fact that over-voltages in power-electronic devices do not only cause sudden failure, but alternatively can initiate a slowly deteriorating condition, which leads to considerably reduced lifetime: Electrical overstress can e.g. cause small internal cracks, which under the impact of humidity can slowly develop into faults.

  For the investigated case of converter failure in wind turbines, this suggests that a lightning event that has led to immediate destruction of one or several converter modules will very probably also have affected the adjacent modules in the converter. These should therefore be expected to have a reduced lifetime. The failure of such pre-damaged modules will then most probably occur at high load and/or severe thermal cycling. In this case, the time-shift between the initiating lightning and the observed failure would mask the correlation between the two events.

  For the future, it is thus recommended to further investigate the presence of electrical-overstress situations, e.g. by means of forensic analysis of failed modules or by means of on-site high-resolution electrical measurements. If the indications obtained in the present study concerning the presence of electric overstress can be confirmed, it is strongly recommended to improve the over-voltage protection in order to ensure that both the power-electronic devices and the control boards are effectively protected from damaging stress levels, to avoid the immediate as well as potential delayed failures.

Within the present project, the analysis of the available data and of converter hardware has provided indications regarding influential external factors and

probable failure mechanisms. Among the large variety of possible failure causes and scenarios, several could be stated to be likely or unlikely.
The objective of future work should be to acquire clear evidence for or against the identified possible failure mechanisms. In order to support this, a more comprehensive collection of converter-failure related data and information is considered crucial. In addition to recording the date of a failure together with the ID of the affected turbine, it is recommended to collect for each converter module

- the module ID,
- the date of installation in the turbine,
- its location (turbine ID, generator-side or grid-side converter),
- the date of failure and
- if possible, information regarding the failure mode (e.g. exploded / not exploded).

This would make it possible to relate pieces of hardware to the turbine they have been operating in as well as to potential grid events or environmental factors at the time of failure. Finally, this would allow the use of more advanced methods of reliability analysis which can e.g. provide evidence for or against the presence of ageing.

In order to gain clearer evidence for or against the relevance of fatigue-related failures in the converter modules, it is recommended that non-destructive Scanning Acoustic Microscopy (SAM) analysis be carried out on larger number of converter-module field returns, and also to include generator-side converter modules. In combination with this, a simplified mechanical testing of the bond wires, as done in the forensic analysis of two modules in the present work, should be carried out. Furthermore, it is recommended that an extended forensic analysis includes micro-sectioning and cross-section inspection of driver-board solder-joints and via-holes, in addition to extended micro-sectioning of chip die-attach and bond-wire connections in the IGBT modules.

Appendix

Table 9: Definition of low-voltage and medium-voltage levels [37]

Region	Relevant Standard	Definition
North America	ANSI C84.1	Low voltage, below 600 V ○ 208 V, 120/240 V, 480 V, 575 V Medium voltage, above 600 V, below 35 kV ○ 2.4 kV, 4.16 kV, 6.9 kV, 12.47 kV, 13.8 kV, 21 kV, 34.5 kV
Europe	IEC 60038	Low voltage, below 1000 V ○ 220 V, 400 V, 690 V Medium voltage, above 1000 V, below 35 kV ○ 3.3 kV, 6.6 kV, 11 kV, 22 kV, 33 kV

References

[1] A. Petersson, T. Thiringer, C. Liljegren, O. Carlson, and S. Lundberg, "Elektriska system i vindkraftverk," Elforsk report 06:04, 2006.

[2] J. Wenske, "Faults of power electronics at harsh environmental conditions within wind-turbine installations," Working document, Fraunhofer IWES, Bremerhaven, 2011.

[3] M. Wilkinson, "Measuring Wind Turbine Reliability, Results Of The Reliawind Project," Presentation at the European Wind Energy Conference & Exhibition EWEA 2011, Brussels, Belgium, 2011.

[4] Hållén and Jonas, ”Vindkraftverket brinner”, Ny Teknik, 2010-04-22.

[5] B. Anjar, M. Dalberg, M. Uppsäll, ”Feasibility study of thermal condition monitoring and condition based maintenance in wind turbines”, Elforsk report 11:19, Stockholm, 2011.

[6] F. Spinato, P.J. Tavner, G.J.W. van Bussel, E. Koutoulakos, "Reliability of wind turbine subassemblies," IET Renewable Power Generation, vol.3, no.4, pp.387-401, December 2009, doi: 10.1049/iet-rpg.2008.0060.

[7] T. Thiringer, J. Paixao, and M. Bongiorno, "Monitoring of the ride-through ability of a 2MW wind turbine in Tvååker, Halland," Chalmers University of Technology, Gothenburg Elforsk report 09:26, 2009.

[8] F. Blaabjerg, Z. Chen, R. Teodorescu, and F. Iov, "Power Electronics in Wind Turbine Systems," in Power Electronics and Motion Control Conference IPEMC 2006, Shanghai, 2006.

[9] U. Scheuermann, “Paralleling of Chips – From the Classical ‘Worst Case’ Consideration to a Statistical Approach”, Proceedings of PCIM 2005, Nuremberg, 2005.

[10] J. Wenske, "Power electronic: Basics, failure mechanisms and modes, reliability", Fraunhofer IWES, Bremerhaven; presentation at Vattenfall, Copenhagen, 10 November 2011.

[11] A. Wintrich, U. Nicolai, W. Tursky, T. Reimann, “Application Manual Power Semiconductors”, Semikron International GmbH, Nuremberg, Germany, 2011.

[12] C. Busca, R. Teodorescu, F. Blaabjerg, S. Munk-Nielsen, P. Rodriguez, L. Helle, T. Abeyasekera, M. Sztykiel, “Press Pack IGBTs: a Reliable Solution for Medium Voltage Multi-Megawatt Wind Turbine Power Converters”. Proceedings of the 10th International Workshop on Large-Scale Integration of Wind Power

into Power Systems as well as Transmission Networks for Offshore Wind Farms. Aarhus, 25-26 November 2011.

[13] M. Boettcher, F. W. Fuchs, "Power Electronic Converters in Wind Energy Systems - Considerations of Reliability and Strategies for Increasing Availability", EPE Joint Wind Energy and T&D Chapters Seminar 2011, 9-11 May 2011.

[14] H. Ye, M. Lin, and C. Basaran, "Failure modes and FEM analysis of power electronic packaging," Finite Elements Anal. Design, vol. 38, pp. 601–612, 2002.

[15] www.solarcompounds.com, accessed March 2012.

[16] F. Lang, U. Scheuermann, "Reliability of spring pressure contacts under environmental stress", Microelectronics Reliability, 47, pp. 1771–1776, 2007.

[17] E. Wolfgang, "Examples for failures in power electronics systems," presented at ECPE Tutorial 'Reliability of Power Electronic Systems.', Nuremberg, Germany, April 2007.

[18] S. Yang, A. Bryant, P. Mawby, D. Xiang, L. Ran, P. Tavner, "An industry-based survey of reliability in power electronic converters," IEEE Transactions on Industry Applications, vol. 47, no. 3, pp. 1441-1451, May/June 2011.

[19] Birk, J.; Andresen, B., "Parallel-connected converters for optimizing efficiency, reliability and grid harmonics in a wind turbine," European Conference on Power Electronics and Applications, 2007, pp.1-7, 2-5 Sept. 2007, doi: 10.1109/EPE.2007.4417318.

[20] Yang, S.; Xiang, D.; Bryant, A.; Mawby, P.; Ran, L.; Tavner, P.: "Condition Monitoring for Device Reliability in Power Electronic vol.25, no.11, pp.2734-2752, Nov. 2010.

[21] Personal communication with H. Ramberg, Volvo Car Corporation, 2011/2012.

[22] Antler, M.: "Contact fretting of electronic connectors", IEICE Trans. Electron., Vol. E82-C, No. 1, January 1999.

[23] E. M. Bock and J. H. Whitley, "Fretting corrosion in electric contacts", AMP Technical Paper P154-74, 1974.

[24] M. Held, P. Jacob, G. Nicoletti, P. Scacco, and M. H. Poech, "Fast power cycling test of IGBT modules in traction application," in Proc. Int. Conf. Power Electron. Drive Syst., 1997, pp. 425–430.

[25] C.Yun, P. Malberti, M. Ciappa, and Fichtner, "Thermal component model for electrothermal analysis of IGBT module systems," IEEE Trans. Adv. Packag., vol. 24, no. 3, pp. 401–406, Aug. 2001.

[26] M. Bartram, "IGBT-Umrichtersysteme fuer Windkraftanlagen: Analyse der Zyklenbelastung, Modellbildung, Optimierung und Lebensdauer-vorhersage, PhD thesis, ISEA, RWTH Aachen, 2005.

[27] Wikipedia, http://en.wikipedia.org/wiki/Whisker_(metallurgy), accessed April 2012.

[28] www.sigcon.com/Pubs/news/10_01.htm, accessed April 2012.

[29] J. Lutz, "Advanced Design with MOSFET and IGBT Power Modules", PCIM conference, Nuremberg, May 2010.

[30] R. Bayerer, T. Herrmann, T. Licht, J. Lutz, M. Feller, "Model for Power Cycling Lifetime of IGBT Modules – Various Factors Influencing Lifetime", Proceedings of the CIPS 2008.

[31] M. Bartram, I. von Bloh, Rik W. De Doncker, "Doubly-Fed Machines in Wind-Turbine Systems: Is this Application Limiting the Lifetime of IGBT Frequency-Converters?", Proceedings of the 351h Annual IEEE Power Electronics Specialists Conference, 2004, pp. 2583-2587.

[32] F. Fuchs, A. Mertens, "Steady state lifetime estimation of the power semiconductors in the rotor side converter of a 2 MW DFIG wind turbine via power cycling capability analysis,", Proceedings of the 14th European Conference on Power Electronics and Applications (EPE 2011), 30 Aug. – 1 Sept. 2011.

[33] S. Konrad, "Ein Beitrag zur Auslegung und Integration spannungsgespeister IGBT-Wechselrichter", PhD thesis, TU Ilmenau, 1997.
[34] K. Xie, Z. Jiang, W. Li, "Effect of Wind Speed on Wind Turbine Power Converter Reliability", IEEE Transactions on Energy Conversion, vol. 27, no. 1, March 2012.

[35] www.mikrotec.dk, visited 2012

[36] G. Wetter, "Failure analysis of converter modules in offshore wind turbines", Report 23551-1, Swerea IVF, Göteborg, August 2012.

[37] Personal communication with H. Zelaya, ABB Corporate Research, 2011.

ELFORSK

SVENSKA ELFÖRETAGENS FORSKNINGS- OCH UTVECKLINGS - ELFORSK - AB

Elforsk AB, 101 53 Stockholm. Besöksadress: Olof Palmes Gata 31
Telefon: 08-677 25 30, Telefax: 08-677 25 35
www.elforsk.se